

Deep Neural Network Concepts for Background Subtraction: A Systematic Review and Comparative Evaluation

Thierry Bouwmans, Sajid Javed, Maryam
Sultana, Soon Ki Jung

Received: date / Accepted: date

Abstract Conventional neural networks show a powerful framework for background subtraction in video acquired by static cameras. Indeed, the well-known SOBS method and its variants based on neural networks were the leader methods on the large-scale CDnet 2012 dataset during a long time. Recently, convolutional neural networks which belong to deep learning methods were employed with success for background initialization, foreground detection and deep learned features. Currently, the top current background subtraction methods in CDnet 2014 are based on deep neural networks with a large gap of performance in comparison on the conventional unsupervised approaches based on multi-features or multi-cues strategies. Furthermore, a huge amount of papers was published since 2016 when Braham and Van Droogenbroeck published their first work on CNN applied to background subtraction providing a regular gain of performance. In this context, we provide the first review of deep neural network concepts in background subtraction for novices and experts in order to analyze this success and to provide further directions. For this, we first surveyed the methods used background initialization, background subtraction and deep learned features. Then, we discuss the adequacy of deep neural networks for background subtraction. Finally, experimental results are presented on the CDnet 2014 dataset.

Thierry Bouwmans
Lab. MIA, Univ. La Rochelle, France
E-mail: tbouwman@univ-lr.fr

Sajid Javed
Dept. of Computer Science, University of Warwick, UK
E-mail: s.javed.1@warwick.ac.uk

Maryam Sultana
Dept. of Computer Science and Engineering, Kyungpook National University, Republic of Korea
E-mail: maryam@vr.knu.ac.kr

Soon Ki Jung
Dept. of Computer Science and Engineering, Kyungpook National University, Republic of Korea
E-mail: skjung@knu.ac.kr

Keywords Background Subtraction · Restricted Boltzmann Machines · Auto-encoders Networks · Convolutional Neural Networks · Generative Adversarial Networks

1 Introduction

In the last two decades, background subtraction for video taken by static cameras has been one of the most active research topics in computer vision due to a big amount of applications including intelligent surveillance as human activities in public spaces, traffic monitoring and industrial machine vision [16, 17, 20, 21, 96]. A big variety of models was used for background/foreground separation such as statistical models [49, 150, 180, 192], fuzzy models [6, 8, 15], subspace learning models [47, 53, 146], robust PCA models [86, 87, 94, 95, 97], and neural networks models [154, 156, 164]. Similarly as PCA models which renewed interest for this task due to the theoretical advances in robust PCA made in 2009 by Candès et al. [26] after an empty period, neural networks progressively renews interest in this field since 2014 [213] due to the practical advances in deep neural networks which are currently usable due to the availability of large-scale datasets [62][203] for the training, and the progress in computational hardware ability¹.

By looking at the story, Schofield et al. [164] were the first authors who used neural networks for background modeling and foreground detection by using a Random Access Memory (RAM) neural networks. But, RAM-NN required that the images represent the background of the scene correctly, and there is not a background maintenance stage because once the RAM-NN is trained with a single pass of background images, it is not possible to modify this information. In a further work, Jimenez et al. [60] classified each zone of a video frame into three classes of background: static, noisy, and impulsive. The classification is performed with a multilayer Perceptron Neural Network which requires a training set from specific zones of each training frame. In another work, Tavakkoli [188] proposed a neural network approach under the concept of novelty detector. During the training step, the background is divided in blocks. Each block is associated to a Radial Basis Function Neural Network (RBF-NN). Thus, each RBF-NN is trained with samples of the background corresponding to its associated block. The decision of using RBF-NN is because it works like a detector and not a discriminant, generating a close boundary for the known class. RBF-NN methods is able to address dynamic object detection as a single class problem, and to learn the dynamic background. However, it requires a huge amount of samples to represent general background scenarios. In Wang et al. [205], a hybrid probabilistic and "Winner Take All" (WTA) neural architectures were combined into a single NN model. The algorithm is named Adaptive Background Probabilistic Neural Network (ABPNN) and it is composed of four layers. In the ABPNN model, each pixel is classified as foreground or background according to a conditional probability of being background. This probability is estimated by a Parzen estimation. The foreground regions are further analyzed in order to classify them as a motion or a shadow region.

¹<https://www.nvidia.fr/deep-learning-ai/>

But, ABPNN needs to define specific initial parameter values (specific thresholds values) for each of the analyzed video. In Culibrk et al. [42], a feed-forward neural network is used for background modeling based on an adaptive Bayesian model called Background Neural Network (BNN). The architecture corresponds to a General Regression Neural Network (GRNN), that works like a Bayesian classifier. Although the architecture is proposed as supervised, it can be extended as an unsupervised architecture in the background model domain. The network is composed of three sub-networks: classification, activation, and replacement. The classifier sub-network maps the features background/foreground of a pixel to a probabilistic density function using the Parzen estimator. The network has two neurons, one of them estimates the probability of being background, and the other neuron computes the probability of being foreground. But, the main disadvantages are that the model is very complex and that it requires of three networks to define if a pixel belongs to the background. In a remarkable work, Maddalena and Petrosino [122] proposed a method called Self Organizing Background Subtraction (SOBS) based on a 2D self-organizing neural network architecture preserving pixel spatial relations. The method is considered as nonparametric, multi-modal, recursive and pixel-based. The background is automatically modeled through the neurons weights of the network. Each pixel is represented by a neural map with $n \times n$ weight vectors. The weights vectors of the neurons are initialized with the corresponding color pixel values using the HSV color space. Once the model is initialized, each new pixel information from a new video frame is compared to its current model to determine if the pixel corresponds to the background or to the foreground. In further works, SOBS was improved in several variants such as Multivalued SOBS [124], SC-SOBS [126], 3dSOBS+ [128], Simplified SOM [27], Neural-Fuzzy SOM [28] and MILSOBS [59]) which allow this method to be in the leader methods on the CDnet 2012 dataset [62] during a long time. SOBS show only interesting performance for stopped object detection [123, 125, 127]. But, one of the main disadvantages of SOBS based methods is the need to manual adjust at least four parameters.

Recently, deep learning methods based on Deep Neural Networks (DNNs) with Convolutional Neural Networks (CNNs also called ConvNets) allow to alleviate the disadvantages of these previous approaches based on conventional neural networks [163][118][66]. While CNNs existed for a long time, their success and then their use in computer vision was limited during a long period due to the size of the available training sets, the size of the considered networks, and the computational capacity. The breakthrough was made by Krizhevsky et al. [104] who used a supervised training of a large network with 8 layers and millions of parameters on the ImageNet dataset [45] with 1 million training images. Since this work, even larger and deeper networks have been trained with the progress made by the storage for Big Data and by the GPUs for deep learning. For the field of background/foreground separation, DNNs were applied with success 1) for background generation [67, 151, 211, 212, 213], 2) for background subtraction [4, 13, 22, 37, 113], 3) foreground detection enhancement [220], 4) for ground-truth generation [204], and 5) for learned deep spatial features [108, 143, 166, 167, 222]. More practically, Restricted Boltzman Machine (RBM) was employed by Guo and Qi [67] and Xu et al. [211] for background generation in order to further achieve moving object detection by background subtraction. In a similar man-

ner, Xu et al. [212,213] used deep auto-encoder networks to achieve the same task while Qu et al. [151] used context-encoder for background initialization. In another approach, Convolutional Neural Networks (CNNs) were employed for background subtraction by Braham and Droogenbroeck [22], Bautista et al. [13], and Cinelli [37]. Other authors employed improved CNNs like Cascaded CNNs [204], deep CNNs [4], structured CNNs [113] and two stage CNNs [226]. In another way, Zhang et al. [222] used Stacked Denoising Auto-Encoder (SDAE) to learn robust spatial features and modeled the background with density analysis whilst Shafiee et al. [166] employed Neural Reponse Mixture (NeREM) to learn deep features used in the Mixture of Gaussians (MOG) model [180]. Motivations and contributions of this paper can be summarized as follows:

- Numerous papers were published in the field of background subtraction since the work of Braham et al. in 2016 showing the big interest of deep neural networks in this field. Furthermore, each new method is in the top algorithms on the CDnet 2014 dataset by offering a big gap of performance compared to conventional approaches. In addition, deep neural networks was also employed in background initialization, foreground detection enhancement, ground-truth generation and deep learned features showing its potential in all the field of background subtraction.
- In this context, we provide an exhaustive comparative survey regarding DNNs approaches used in the field of background background initialization, background subtraction, foreground detection and features. For this, we compare them in terms of architecture and performance.

The rest of this paper is as follows. First, we provide in Section 2 a short reminder on the different key points in deep neural networks for novices. In Section 3, we review the methods based on deep neural networks for background generation in video. In Section 4, we provide the methods based on deep neural networks for background subtraction with a full comparative overview in terms of architecture and challenges. In Section 5, deep learned features in this field are surveyed. In addition, we also provide a discussion about the adequacy of deep neural networks for background subtraction. Finally, experimental results are presented on the CDnet 2014 dataset in Section 7, and concluding remarks are given in Section 8.

2 Deep Neural Networks: A Short Overview

2.1 Story Aspects

DNN recently emerges from a long history of neural networks with two empty periods. Since its beginning, more and more sophisticated concepts and related architectures were developed for neural networks and after for deep neural networks. Full surveys were provided by Schmidhuber [163] in 2015, Yi et al. [217] in 2016, Liu et al. [118] in 2017, and Gu et al. [66] in 2018. In addition, a full description of the different DNN concepts are available at the Neural Network Zoo website². Here we briefly summarize the main steps of the DNN's story. DNN begins in 1943 with the threshold logic unit (TLU) [132]. In further works, Rosenblatt [159] designed the first

perceptron in 1957 whilst Widrow [207][208] developed the Adaptive Linear Neuron (ADALINE) in 1962. This first generation of neural networks are fundamentally limited in what they can learn to do. During the 1970s (first empty period), research focused more on XOR problem. The next period concerns the emergence of more advanced neural networks like multilayer back-propagation neural networks, Convolutional Neural Networks (CNNs), and Long Short-Term Memory (LSTMs) for Recurrent Neural Networks (RNNs) [80]. This second generation of neural networks mostly used back-propagation of the error signal to get derivatives for learning. After 1995 until 2006 (second empty period), research focused more Support Vector Machine (SVM) which is a very clever type of perceptron developed by Vapnik et al. [39]. Thus, many researchers abandoned neural networks research with multiple adaptive hidden layers because SVM worked better with less computational time requirements and training. With the progress of GPU and the storage of Big Data, DNN regains attention and developments with new deep learning concepts such as a) Deep Belief Networks [79][78] in 2006 and b) Generative Adversarial Networks (GANs) [50][162] in 2014. Liu et al. [118] classified the deep neural network architectures in the following categories: restricted Boltzmann machines (RBMs), deep belief networks (DBNs), autoencoders (AEs) network and deep Convolutional Neural Network (CNNs). In addition, deep probabilistic neural networks [58], deep fuzzy neural networks [46][54] and Generative Adversarial Networks (GANs) [50][162] can also be considered as other categories. Applications of these deep learning architecture are mainly in speech recognition, computer vision and pattern recognition [118]. In this context, DeepNets architectures for specific applications have emerged such as the following well-known architecture: AlexNet developed by Krizhevsky et al. [104] for image classification in 2012, VGG-Net designed by Simonyan and Zisserman [175] for large-scale image recognition in 2015, U-Net [158] developed by Ronneberger et al. [158] for biomedical image segmentation in 2015, GoogLeNet with inception neural network introduced by Szegedy et al. [184] for computer vision in 2015, and Microsoft Residual Network (ResNet) designed by He et al. [73] for image recognition in 2016. Thus, all the current architectures were designed for a target application like speech recognition [144], computer vision [63] and pattern recognition [118] which its specific features giving very impressive performance in comparison on the previous state-of-art methods based on GMM and graph-cut as in the problem of foreground detection/segmentation/localization.

2.2 Features Aspects

As seen in the previous part, DNNs are determined by their architecture that becomes more and more sophisticated over time. Practically, an architecture consists of different layers classified as input layer, hidden layer and output layer. Each layers contains a number of neurons that are activated or not following an activation function. This activation function can be viewed as the mapping of the input to the output via a non-linear transform function at each node. In literature, different activation functions can

²<http://www.asimovinstitute.org/neural-network-zoo/>

be found as the sigmoid function [48], Rectified Linear Unit (ReLU) [148], and Probabilistic ReLU (PReLU) [74]. Once the architecture is determined and the activation function is chosen, the DNN need to be trained using a large-scale dataset such as ImageNet dataset [104], CIFAR-10 dataset and ILSVRC 2015 dataset for classification tasks. For this, the architecture is exposed to the training dataset to learn the weights of each neurons in each layer. The parameters are learned via a cost function that are minimized on the desired output and the predicted one. The most common method for training is the back-propagation. Usually, the gradient of the error function computed on the correct output and the predicted one is propagated back to the beginning of the network in order to update its parameters. For this, it requires a gradient descent algorithm. Batch normalization which normalizes mini-batches can also be used to accelerate learning because it employs higher learning rates, and also regularizes the learning. For vocabulary, an epoch is a complete pass through a given dataset, and thus is the number of time where the neural network has been exposed to every record of the dataset once. An epoch is not an iteration which corresponds to one update of the neural net models parameters. Many iterations can occur before an epoch is over. Epoch and iteration are only identical if the parameters are updated once for each pass through the whole dataset.

2.3 Theoretical Aspects

Theoretical aspects concern mainly the understanding and the provability of DNNs [145, 194, 195, 219], but also their properties in presence of adversarial perturbations [34, 137, 138, 139, 140, 186, 231], and their robustness in presence of noisy labels [189]. For this, the principle key features to design DNNs need to be mathematically investigated as follows [194, 195]:

- **Architecture:** The number, the size and the type of the layers are key characteristics of an architecture as well as the classes of functions that can be approximated by a feed-forward neural network. The key issue is how the chosen architecture impact expressiveness.
- **Optimization:** It concerns the way to train the DNNs. This issue contains two aspects which are the datasets used for the training, and mostly the algorithm to optimize the network. The problem is generally non-convex, and following the appearance of the error surface how to guarantee the optimality and when does descent gradient succeed? Is "the local minima are global property" hold for deep nonlinear networks?
- **Generalization:** How well do DNNs generalize? How should DNNs be regularized? How to prevent under and over fitting?

Both architecture and optimization can impact generalization [145, 194, 195, 219]. Furthermore, several architectures are easier to optimize than others [194, 195]. First replies about the global optimality can be found in Yun et al [219]. In addition, Wang et al. [197] show that deep neural networks can be better understood by utilizing the knowledge obtained by the visualization of the output images obtained at each layers. Other authors provided either a theoretical analysis or visualizing analysis in a

context of an application. For example, Basu et al. [12] published a theoretical analysis for texture classification whilst Minematsu et al. [134, 135] provided a visualizing analysis for background subtraction. Despite these first valuable investigation, the understanding of DNNs remains still shallows. Nevertheless, DNNs have been applied with success in many computer vision applications gaining a big gap of performance. This success is intuitively due to the following reasons: 1) features are learned rather than manual hand-crafted, 2) more layers capture more invariance, 3) more data allow a deeper training, 4) more computing CPU, 5) better regularization (Dropout [177]) and 6) new non-linearity (max-pooling, ReLU [142]).

2.4 Implementation Aspects

For software implementation, many libraries for the development in different programming languages are available to implement DNNs. The most known libraries are Caffe [98], MatConvNet [193] from Matlab, Microsoft Cognitive Toolkit (CNTK), TensorFlow [51], Theano³ and Torch⁴. All these software support interfaces of C, C++ and/or Python for quick development. For a full list, the reader are referred to go on the deeplearning.net⁵ website. There is also a Deep Learning library for Java (DL4J⁶). For hardware implementation and optimization, there are several designed GPUs from NVIDIA with dedicated SDKs⁷. For example, the deep learning GPU Training System (DIGITS⁸) provides fast training of DNNs for computer vision applications like image classification, segmentation and object detection tasks whilst NVIDIA Jetson is designed for embedded systems. For NVIDIA Volta GPUs, TensorRT protect⁹ allow to optimize deep learning inference and runtime. It also allows to deploy trained neural networks for inference to hyper-scale data centers or embedded. Deep neural network accelerator based on FPGA also existed [84].

In the following sections, we survey all the previous DNN approaches used in background/foreground separation steps by comparing their advantages and disadvantages as well as their performance on the CDnet 2014 dataset.

3 Background Generation

Background generation [18, 100, 129] (also called background initialization [89, 91] [92, 176], background estimation [38, 70], and background extraction [198]) regards the initialization of the background. Generally, the model is often initialized using the first frame or a background model over a set of training frames which contain or do

³<http://deeplearning.net/software/theano/>

⁴<http://torch.ch/>

⁵<http://deeplearning.net/software-links/>

⁶<https://deeplearning4j.org/>

⁷<https://developer.nvidia.com/deep-learning-software>

⁸<https://developer.nvidia.com/digits>

⁹<https://developer.nvidia.com/tensorrt>

Categories	Methods	Authors - Dates
Restricted Boltzmann Machines	Partially-Sparse RBM (PS-RBM) Temp. Adaptive RBM (TARBM) Gaussian-Bernoulli RBM RBM (PTZ Cameras)	Guo and Qi [67] (2013) Xu et al. [211] (2015) Sheri et al. [171] (2018) Rafique et al. [153] (2014)
Deep Auto-encoders Networks	Deep Auto-encoder Networks (DAN) DAN with Adaptive Tolerance Measure Encoder-Decoder CNN (ED-CNN)	Xu et al. [213] (2014) Xu et al. [212] (2014) Qu et al. [151] (2016)
Convolutional Neural Networks	FC-Flownet BM-Unet	Halfaoui et al. [70] (2016) Tao et al. [187] (2017)
Generative Adversarial Networks	Deep Context Prediction (DCP) ForeGAN-RGBD	Sultana et al. [181] (2018) Sultana et al. [182] (2018)

Table 1 Deep Neural Networks in Background Generation: An Overview

not contain foreground objects. This background model can be the temporal average or the the temporal median. But, it is impossible in several environments due to bootstrapping and then it needs a sophisticated model to construct this first image. The top algorithms on the SBMnet dataset are the algorithms named Motion-assisted Spatio-temporal Clustering of Low-rank (MSCL) [93] and LaBGen [105, 106, 107] that are based on robust PCA [20, 21] and the robust estimation of the median, respectively. Practically, the main challenge is to obtain a first background model when more than half of the training contains foreground objects. This learning process can be done off-line and so the algorithm can be a batch one. Thus, deep neural networks are suitable for this task and several DNN methods have been recently used in this field. We have classified them in the following categories and Table 1 shows an overview of these methods. In addition, the list of publications is available at the Background Subtraction Website¹⁰ and is regularly updated.

3.1 Restricted Boltzmann Machines (RBMs)

Guo and Qi [67] were the first authors who applied Restricted Boltzmann Machine (RBM) to background generation by using a Partially-Sparse RBM (PS-RBM) framework in order to detect moving objects by background subtraction. This framework models the image as the integration of RBM weights. By introducing a sparsity target, the learning process alleviate the tendency of growth in weights. Once the sparse constraints are added to the objective function, the hidden units only keep active in a rather small portion on the specific training data. In this context, Guo and Qi [67] proposed a controlled redundancy technique, that allow the hidden units to learn the distinctive features as sparse as possible, meanwhile, the redundant part rapidly learns the similar information to reduce the total error. The PS-RBM provides accurate background modeling even in dynamic and noisy environments. Practically, PS-RBM provided similar results than DPGMM [69], KDE [49], KNN [234], and SOBS [122] methods on the CDnet 2012 dataset.

¹⁰<https://sites.google.com/site/backgroundsubtraction/background-initialization/neural-networks>

In a further work, Xu et al. [211] proposed a Temporally Adaptive RBM (TARBM) background subtraction to take into account the spatial coherence by exploiting possible hidden correlations among pixels while exploiting the temporal coherence too. As a result, the augmented temporally adaptive model can generate more stable background given noisy inputs and adapt quickly to the changes in background while keeping all the advantages of PS-RBM including exact inference and effective learning procedure. TARBM outperforms the standard RBM, and it is robust in presence of dynamic background and illumination changes.

Sheri et al. [171] employed a Gaussian-Bernoulli restricted Boltzmann machine (GRBM) which is different from the ordinary restricted Boltzmann machine (RBM) by using real numbers as inputs. This network results in a constrained mixture of Gaussians, which is one of the most widely used techniques to solve the background subtraction problem. Then, GRBM easily learn the variance of pixel values and takes the advantage of the generative model paradigm of the RBM.

In the case of PTZ cameras, Rafique et al. [153] modeled the background scene by using RBM. The generative modeling paradigm of RBM gives an extensive and nonparametric background learning framework. Then, RBM was trained with one step contrastive divergence.

3.2 Deep Auto Encoder Networks (DAE)

Xu et al. [213] designed a background generation method based on two auto-encoder neural networks. First, the approximate background images are computed via an auto-encoder network called Reconstruction Network (RN) from the current video frames. Second, the background model is learned based on these background images with another auto-encoder network called Background Network (BN). In addition, the background model is updated on-line to incorporate more training samples over time. Experimental results on the I2R dataset [109] show that DAN outperforms MOG [180], Dynamic Group Sparsity (DGS) [83], Robust Dictionary Learning (RDL) [225] and Online RDL (ORDL) [121]. In a further work, Xu et al. [212] improved this method by using an Adaptive Tolerance Measure. Thus, DAN-ATM can handle large variations of dynamic background more efficiently than DAN. Experimental results on the I2R dataset [109] confirm this gap of performance.

Qu et al. [151] employed a context-encoder network for a motion-based background generation method by removing the moving foreground objects and learning the feature. After removing the foreground, a context-encoder is also used to predict the missing pixels of the empty region, and to generate a background model of each frame. The architecture is based on the AlexNet architecture that produces a latent feature representation of input image samples with empty regions. The decoder has five up convolutional layers, and uses the feature representation to fill the missing regions of the input samples. The encoder and the decoder are connected through a channel-wise fully connected layer. It allows information to be propagated within activations of each feature map. Experiments provided by Qu et al. [151] are limited but convincing.

3.3 FC-FlowNet

Halfaoui et al. [70] employed a CNN architecture for background estimation which can provide a background image with just a small set of frames containing foreground objects. The CNN is trained estimate background patches and then it is followed by a post-processing step to obtain the final background image. The architecture is based on FlownetSimple [56] which is a two-stage architecture developed for the prediction of the optical flow motion vectors. The first stage is a contractive stage whilst the a second one is a refinement stage. The contractive stage is a succession of convolutional layers. This rather generic stage extracts high level abstractions of the stacked input images, and forwards the gained feature maps to the up convolutional refinement stage, in order to enhance the coarse-to-fine transformations. Halfaoui et al. [70] adapted this architecture by providing a Fully-concatenated version called FCFlowNet. Experimental results [70] on the SBMC 2016 dataset¹¹ demonstrates robustness against very short or long sequences, dynamic background, illumination changes and intermittent object motion.

3.3.1 U-Net

Tao et al. [187] proposed an unsupervised deep learning model for Background Modeling called BM-Unet. This method is based on the generative architecture U-Net [158] which for a given frame (input) provides the corresponding background image (output) with a probabilistic heat map of the color values. In addition, this method learns parameters automatically and uses intensity differences and optical flow features in addition of color features to tackle camera jitter and quick illumination changes Besides, BM-Unet can be applied on a new video sequence without the need of re-training. Practically, Tao et al. [45] proposed two algorithms named Baseline BM-Unet and Augmented BM-Unet that can handle static background and background with illumination changes and camera jitter, respectively. The BM-Unet is based on the so called guide features which are used to guide the network to generate the background corresponding to the target frame. Experimental results [187] on the SBMnet dataset¹² [100] demonstrate promising results over neural networks methods (BEWiS [64], BE-AAPSA [155], and FC-FlowNet [70]), and state-of-the-art methods (Photomontage [1], LabGen-P [105]).

3.4 Generative Adversarial Networks (GANs)

Generative Adversarial Networks (GAN) have been a breakthrough in machine learning. Introduced in 2014, GAN [50][162] provide a powerful framework for using unlabeled data to train machine learning models, rising as one of the most promising paradigms for unsupervised learning. Based on GAN, Sultana et al. [181] designed

¹¹<http://pione.dinf.usherbrooke.ca/sbmc2016/>

¹²<http://scenebackgroundmodeling.net/>

Categories	Methods	Authors - Dates
Convolutional Neural Networks	CNN (ConvNets) CNN (ConvNets) CNN (ConvNets) (Analysis) (2) CNN (Pedestrian Detection) CNN (GoogLeNet) CNN (RPaTP feature) CNN (Depth feature)	Braham and Van Droogenbroeck [22] (2016) Bautista et al. [13] (2016) Minematsu et al. [134] (2017) Yan et al. [214] (2018) Weinstein [206] (2018) Zhao et al. [224] (2018) Wang et al. [201] (2018)
Multi-scale and Cascaded CNN	Cascaded CNN (Ground-Truth) FgSegNet-M FgSegNet-S FgSegNet-V2 MCSS Guided Multi-scale CNN	Wang et al. [110] (2016) Lim and Keles [114] (2018) Lim and Keles [115] (2018) Lim et al. [116] (2018) Liao et al. [112] (2018) Liang et al. [111] (2018)
Fully CNNs	Basic Fully CNN Basic Fully CNN Multiview recep. field FCN (MV-FCN) Multiscale Fully CNN (MFCN) CNN-SFC (Foreground Masks) Fully Conv. Semantic Net. (FCSN)	Cinelli [37] (2017) Yang et al. [216] (2017) Akilan et al. [2] (2018) Zeng and Zhu [221] (2018) Zeng et al. [220] (2018) Lin et al. [117] (2018)
Deep CNN	Deep CNNs TCNN/Joint TCNN Adaptive deep CNN (ADCNN) SPFN	Babae et al. [4] (2017) Zhao et al. [226] (2017) Li et al. [110] (2018) Chen et al. [32] (2018)
Structured CNN	Struct CNNs	Lim et al. [113] (2017)
3D CNNs	3D-CNNs STA-3D ConvNets (ReMoteNet) 3D Atrous CNN (ConvLSTM)	Sakkos et al. [161] (2017) Yu et al. [218] (2017) Hu et al. [82] (2018)
Generative Adversarial Networks	BScGAN Bayesian GAN (BGAN) Bayesian Parallel Vision GAN (BPVGAN) Neural Unsupervised Moving Object Detection (NUMOD)	Bakkay et al. [10] (2018) Zheng et al. [228] (2018) Zheng et al. [230] (2018) Bahri et al. [9] (2018)

Table 2 Deep Neural Networks in Background Subtraction: An Overview

an unsupervised Deep Context Prediction (DCP) for background initialization in the context of background/foreground separation. Practically, DCP is an unsupervised visual feature learning hybrid GAN based on context prediction. It is followed by a semantic inpainting network for texture optimization. Sultana et al. [181] trained the context prediction model additionally with scene-specific data in terms of patches of size 128×128 for 3 epochs. The texture optimization is done with VGG19 network pre-trained on ImageNet [45] for classification. Then, the frame selection for inpainting the background is done by summation of pixel values in the forward frame difference technique. If the sum of difference pixels is small, then current frame is selected. Experimental results on the SBM.net dataset [100] show that DCP achieved an average gray level error to be 8.724 which is minimum among all the compared low-rank methods, that are RFSA [68], GRASTA [72], GOSUS [210], SSGoDec [232], and DECOLOR [233]. In a further work, Sultana et al. [182] extended this method to RGB-D videos by separately training two DCPs: one for RGB videos and one for depth videos. Then, each generated background sample is then subtracted from the given test sample to detect foreground objects either in RGB or in depth. Finally, the final foreground mask is obtained by combining the two foreground masks with a logical AND. Experiments on the SBM- RGBD¹³ dataset [25] show that ForeGAN-RGBD model outperforms cwisardH+ [65], RGB-SOBS [126], and SRPCA [90] with an average F-Measure of 0.8966.

¹³<http://rgb2017.na.icar.cnr.it/SBM-RGBDdataset.html>

Methods	Input	Output	Architecture Encoder/Decoder	Additional Architecture	Activation Function	Conv. Layers	Fully Conv.	Implementation Framework
Basic CNNs								
ConvNets [22]	Backg. (Median) Current Image	Foreground	LeNet-5 [43]	-	ReLU/Sigm.	2	1	-
Basic CNNs [110]	Current Image	Foreground	CNN-1	-	ReLU/Sigm.	4	2	Caffe [98]/MatConvNet [193]
Basic CNNs [214]	Backg. Visible (Median) Backg. Thermal (Median) Current Image (Visible) Current Image (Thermal)	GT	CNN	-	ReLU/Sigm.	4	-	-
Basic CNNs [206]	Backg. (Median) Current Image	Foreground (Bound. Box)	GoogLeNet [184]	-	ReLU/Sigm.	-	-	Tensorflow [51]
Basic CNNs [224]	Current Image (RPoTP)	Foreground	CNN	-	ReLU	-	1	-
Basic CNNs [201]	Background Image (Average) (Depth) Current Image (Depth)	Foreground	CNN	(MLP)	ReLU/Sigmoid	3	3	-
Multi-scale and Cascaded CNNs								
Multi-scale CNNs [110]	Current Image	GT	CNN-1	-	ReLU/Sigm.	-	-	Caffe [98]/MatConvNet [193]
Cascaded CNNs [110]	Current Image	GT	CNN-1	CNN-2	ReLU/Sigm.	-	-	Caffe [98]/MatConvNet [193]
FgSegNet-M [114]	Current Image	Foreground	VGG-16 [175]	TCNN	ReLU/Sigm.	4	-	Keras [36]/TensorFlow [51]
FgSegNet-S [115]	Current Image	Foreground	VGG-16 [175]	TCNN/FPM	ReLU/Sigm.	4	-	Keras [36]/TensorFlow [51]
FgSegNet-V2 [116]	Current Image	Foreground	VGG-16 [175]	TCNN/FPM Feat. Fusions	ReLU/Sigm.	4	-	Keras [36]/TensorFlow [51]
MCSS [112]	Backg. Current Image	Foreground	ConvNets [22]	-	ReLU/Sigm.	2	2	-
Guided Multi-scale CNN [111]	Current Image	Foreground	ConvNets [22]	Guided Learning	ReLU/Sigm.	4	-	-
Fully CNN								
Fully CNNs [37]	Backg. (Median) Current Image	Foreground	LeNet-5 [43]	-	ReLU/Sigm.	4	-	Torch7
Fully CNNs [37]	Backg. (Median) Current Image	Foreground	ResNet [76]	-	ReLU/Sigm.	-	-	Torch7
Deep FCNNs [216]	Current Image	Foreground	Multi. Branches (4)	CRF	PReLU [74]	5 (Atrous)	1	-
MV-FCN [2]	Current Image	Foreground	U-Net [158]	2CFs/PFF	ReLU/Sigm.	1 (2D Conv.)	1	Keras/Python
MFCN [221]	Current Image	Foreground	VGG-16 [175]	-	ReLU/Sigm.	5	-	TensorFlow [51]
CNN-SFC [220]	3 For. Masks	Foreground	VGG-16 [175]	-	ReLU/Sigm.	13	None	TensorFlow [51]
FCSN [117]	Backg. (SubSENSE) Current Image	Foreground	FCN/VGG-16 [119]	-	ReLU/Sigm.	20	3	TensorFlow [51]
Deep CNNs								
Deep CNN [4]	Backg. (SubSENSE /FTSG) Current Image	Foreground	CNN	Multi-Layer Perceptron (MLP)	ReLU/Sigm.	3	-	-
TCNN/Joint TCNN [226]	Backg. Current Image	Foreground	MCFC (VGG-16)	DCGAN [152]/ Context Enc. [147]	ReLU/Sigm.	-	-	Caffe [98]/DeepLab [29]
ADCNN [110]	Current Image	Foreground (Bound. Box)	T-CNN	-	ReLU/Sigm.	7	None	Caffe [98]
SFEN [32]	Current Image	Foreground	S-CNN, C-CNN VGG-16 GoogLeNet [184] ResNet	Attention ConvLSTM/ STN/CRF	ReLU/Sigm.	-	-	-
Structured CNN								
Struct CNN [113]	Back. (Median) Current Image t Image t-1	Foreground	VGG-16	-	PReLU [74]	13	-	Caffe [98]
3D CNNs								
3D ConvNet [161]	10 Frames	Foreground	C3D Branch [190]	-	-	6 (3D Conv.)	-	Caffe [98]
STA-3D ConvNets (ReMoteNet) [218]	Current Image	Foreground (Bound. Box)	Modified C3D Branch [218]	ST Attention ConvLSTM	ReLU	(3D Conv.)	-	TensorFlow [51]
3D Atrous CNN [2]	Current Image	Foreground	3D Atrous ConvLSTM	-	ReLU	5 (3D Conv.)	-	TensorFlow [51]
Generative Adversarial Networks								
BScGAN [10]	Back. (Median) Current Image	Foreground	cGAN [85]	-	Leaky ReLU/Tanh Leaky ReLU/Sigm	8 4	- -	Pytorch Pytorch
BGAN [228]	Back. (Median) Current Image	Foreground	Bayesian GAN	-	-	-	-	-
BPVGAN [228]	Back. (Median) Current Image	Foreground	Paralell Bayesian GAN	-	-	-	-	-
NUMOD [9]	Current Image Illum. Image Foreground	Back.	GFCN Bayesian GAN	-	ReLU/Sigm.	-	-	-

Table 3 Deep Neural Networks Architecture in Background Subtraction: A Comparative Overview. “-” stands for “not indicated” by the authors.

Methods	Multi-scale (Size)	Training (Over-fitting)	Training (GT)	Spatial (Pixel)	Computation	End-to-End	Long-Term (Temporal)	Features	Type
Basic CNNs									
ConvNets [22]	No (27 × 27)	Scene-specific	GT/IUTIS	No	Yes	No (Pre-proc.)	No	Grey	Generator
Basic CNNs [214]	No (64 × 64)	Scene-specific	GT	No	No	No (Pre-proc.)	No	RGB/IR	Generator
Basic CNNs [110]	No (31 × 31)	Scene-specific	GT	No	Yes	Yes	No	RGB	Generator
Basic CNNs [224]	Frame	-	one GT	No	-	No (RPoTP)	Yes	RPoTP feature [224]	Generator
Basic CNNs [201]	Patch	-	GT (SBM-RGBD)	No	No	No (Pre-process.)	Np	Depth feature	Generator
Multi-scale and Cascaded CNNs									
Multi-scale CNNs [110]	3 scales	Scene-specific	GT	Cascaded (2)	Yes	Yes	No	RGB	Generator
Cascaded CNNs [110]	3 scales	Scene-specific	GT	Cascaded (2 levels)	Yes	Yes	No	RGB	Generator
FgSegNet-M [114]	3 scales	Imbalanced data	GT	TNN	18 fr/s	Yes	No	RGB	Generator
FgSegNet-S [115]	FPM	Imbalanced data	GT	TNN	-	Yes	No	RGB	Generator
FgSegNet-V2 [116]	M-FPM	Imbalanced data	GT	TNN	-	Yes	No	RGB	Generator
MCS5 [112]	3 scales (27 × 27)	Scene-specific	GT (Small Number)	Cascaded (2 levels)	-	Yes	No	Grey	Generator
Guided Multi-scale [111]	3 scales (31 × 31)	Scene-specific	GT	-	-	No (Post-proc.)	No	RGB	Generator
Fully CNNs									
Fully CNNs [37]	No	Scene-specific	GT	No	Yes	Yes	No	Grey	Generator
Deep FCNNs [216]	No	-	GT	Atrous	Yes	Yes	No	-(RGB?)	Generator
MV-FCN [2]	Inception Mod.	-	GT	-	-	Yes	Encoder	-(RGB?)	Generator
MFCN [221]	Yes (224 × 244 × 3)	-	Mean	-	27 fr/s	Yes	No	Infrared	Generator
	Yes (224 × 244 × 3)	-	Mean	-	-	Yes	No	RGB	Generator
CNN-SFC [220]	No	No	GT	No	No	No	No	Black/White	Generator
FCSN [117]	Semantic	No	GT/SuBSENSE	Semantic	48 fr/s	Yes	No	-(RGB?)	Generator
Deep CNNs									
Deep CNN [4]	No (37 × 37)	Scene-specific	GT	No	Yes	No (Post-proc.)	No	RGB	Generator
TCNN/Joint TCNN [226]	Yes (961 × 961)	Background Generation	GT	No	5 fr/s	Yes	No	RGB	Generator
ADCNN [110]	Atrous Sampling Rate	Discriminative Features	GT	No	-	Yes	No	RGB	Generator
	Yes		(CUHK, MIT, PETS)						
SFEN [32]	Semantic	No	GT	STN	15 fr/s	Yes	No	RGB	Generator
SFEN+CRF [32]	Semantic	No	GT	STN/CRF	6 fr/s	Yes	No	RGB	Generator
SFEN+PSL+CRF [32]	Semantic (224 / <i>times</i> 224)	No	GT	STN/CRF/PSL	5 fr/s	Yes	ConvLSTM	RGB	Generator
Structured CNNs									
Struct CNN [113]	Contours (336 × 336)	No	GT	Superpixel	-	No (Post-proc.)	No	Grey	Generator
3D CNNs									
3D ConvNet [161]	Multi-kernel upsampling	Yes	GT	No	-	Yes	3D	-(RGB?)	Generator
STA-3D ConvNets (ReMoteNet) [218]	1280 × 720)	No	GT	STA ConvLSTM	Fast	Yes	STA ConvLSTM	RGB	Generator
3D Atrous CNN [2]	320 × 240)	No	GT	Atrous	-	Yes	3D/ConvLSTM	-(RGB?)	Generator
Generative Adversarial Networks									
BScGAN [10]	256 × 256)	No	GT	No	10 fr/s	Yes	No	-(RGB?)	Generator/Discriminator
BGAN [228]	-	-	GT	-	-	Yes	-	-	Generator/Discriminator
BPVGAN [228]	-	-	GT	-	Parallel Implem.	Yes	-	-	Generator/Discriminator
NUMOD [9]	Frame	No	$I = B + C + F$	No	-	Yes	No	RGB	Generator/

Table 4 Deep Neural Networks in Background Subtraction: A Comparative Overview for Challenges. ”-” stands for ”not indicated” by the authors.

4 Background Subtraction

Background subtraction consists of comparing the background image with the current image to label pixels as background or foreground pixels. The top algorithms on the large-scale dataset CDnet 2014 are three DNNs based methods (FgSegNet [113], BSGAN [229], Cascaded CNN [204]) for supervised approaches followed by three no-supervised methods that are multi-features/multi-cues approaches (SuB-SENSE [178], PAWCS [179], IUTIS [14]). This task is a classification one, that can be achieved with success by DNN. For this, different methods have been developed in literature and we review them in the following sub-sections. Table 2 shows an overview of these methods. In addition, the list of publications is available at the Background Subtraction Website¹⁴ and is regularly updated.

4.1 Convolutional Neural Networks

Braham and Van Droogenbroeck [22] were the first authors to use Convolutional Neural Networks (CNNs) for background subtraction. This model named ConvNet has a similar structure than LeNet-5 [43]. Thus, the background subtraction model involves four stages: background image extraction via a temporal median in grey scale, specific-scene dataset generation, network training and background subtraction. More precisely, the background model is built for a specific scene. For each frame in a video sequence, image patches that are centered on each pixel are extracted and then they are combined with corresponding patches from the background model. Braham and Van Droogenbroeck [22] used a patch size of 27×27 . After, these combined patches are fed to the network to predict probability of foreground pixels. For the architecture, Braham and Van Droogenbroeck [22] employed 5×5 local receptive fields, and 3×3 non-overlapping receptive fields for all pooling layers. The first and second convolutional layers have 6 and 16 feature maps, respectively. The first fully connected layer has 120 hidden units and the output layer consists of a single sigmoid unit. The algorithm needs for training the foreground results of a previous segmentation algorithm named IUTIS [14] or the ground truth information provided in CDnet 2014 [203]. Half of the training examples are used for training ConvNet and the remaining frames are used for testing. By using the results of the IUTIS method [14], the segmentation produced by the ConvNet is very similar to other state-of-the-art methods whilst the algorithm outperforms all other methods significantly when using the ground-truth information especially in videos of hard shadows and night videos. With the CDnet2014 dataset (excluding the IOM and PTZ categories), this method with IUTIS and GT achieved an average F-Measure of 0.7897 and 0.9046, respectively. Baustita et al. [13] also used a simple CNN but for the specific task of vehicle detection. For pedestrian detection, Yan et al. [214] employed the similar scheme with both visible and thermal images. Then, the inputs of the network have a size of $64 \times 64 \times 8$ which includes the visible frame (RGB), thermal frame (IR), visible background (RGB) and thermal background (IR). The outputs of the network have a size of $64 \times 64 \times 2$. Experiments on OCTBVS dataset¹⁵ show that this method

¹⁴<https://sites.google.com/site/backgroundsubtraction/recent-background-modeling/deep-learning>

outperforms T2-FMOG [8], SuBSENSE [178], and DECOLOR [233]. For biodiversity detection in terrestrial and marine environments, Weinstein [206] employed the GoogLeNet architecture integrated in a software called DeepMeerkat¹⁶. Experiments on humming bird videos show robust performance in challenging outdoor scenes where moving foliage occur.

Remarks: ConvNet is the simplest manner to learn the differences between the background and the foreground via CNNs. Thus, the work of Braham and Van Droogenbroeck [22] presents the very big merit to be the first application of deep learning for background subtraction, and can then be used as a reference for comparison in terms of improvements and performance. But, it presents several limitations: 1) It is difficult to learn the high-level information through patches [117]; 2) due to the over-fitting that is caused by using highly redundant data for training, the network is scene-specific. In practice, it can only process a certain scenery, and needs to be retrained for other video scenes [4]. This fact is not a problem most of the time because the camera is fixed filming always similar scenes. But, it may not be the case in certain applications as pointed out by Hu et al. [82]. ; 3) Each pixel is processed independently and then the foreground mask may contain isolated false positives and false negatives; 4) It is computationally expensive due to large number of patches extracted from each frame as remarked by Lim and Keles [114]; 5) it requires pre-processing or post-processing of the data, and hence is not based on an end-to-end learning framework [82]; 6) ConvNet use few frames as input and thus can not consider long-term dependencies of the input video sequences [82]; and 7) ConvNet is a deep encoder-decoder network that is a generator network. But, the classical generator networks produce blurry foreground regions and such networks can not preserve the objects edges because they minimize the classical loss functions (e.g., Euclidean distance) between the predicted output and the ground-truth [117]. Since this first valuable work, the posterior methods developed in the literature attempt to alleviate these limitations that are the main challenges to use DNN in background subtraction. Table 3 shows a comparative overview with all the posterior methods while Table 4 show an overview in terms of the challenges. These tables are discussed in Section 6.

4.2 Multi-scale and Cascaded CNNs

Wang et al. [204] proposed a deep learning method for an iterative ground-truth generation process in the context of background modeling algorithms validation. In order to yield the ground truths, this method segments the foreground objects by learning the appearance of foreground samples. First, Wang et al. [204] designed basic CNN and the multi-scale CNN which processed each pixel independently based on the information contained in their local patch of size 31×31 in each channel RGB. The basic CNN model consists of 4 convolutional layers and 2 fully connected layers. The first 2 convolutional layers come with 2×2 max pooling layer. Each convolutional layer uses a filter size of 7×7 and Rectified Linear Unit (ReLU) as the activation function.

¹⁵<http://vcipl-okstate.org/pbvs/bench/>

¹⁶<http://benweinstein.weebly.com/deepmeerkat.html>

By considering the CNN output as a likelihood probability, a cross entropy loss function is employed for training. Because, this basic model processes patches of size 31×31 , its performance is limited to distinguish foreground and background objects with the same size or less. This limitation is alleviated by the multi-scale CNN model which gives three outputs of three different sizes further combined in the original size. In order to model the dependencies among adjacent pixels and thus enforce spatial coherence, Wang et al. [204] employed the multi-scale CNN model with a cascaded architecture that is named Cascaded CNN. Practically, the CNN presents the advantage of learning or extracting its own features that may be better than hand-designed features. The CNN is fed with manually generated foreground objects from some frames of a video sequence to learn the foreground features. After this step, the CNN employs generalization to segment the remaining frames of the video. Wang et al. [204] trained scene specific networks using 200 frames by manual selection. Cascaded CNN provides an overall F-Measure of 0.9209 in CDnet2014 dataset [203]. For the Cascaded CNN's implementation¹⁷ available online, Wang et al. [204] used the Caffe library¹⁸ [98] and MatConvNet¹⁹. The limitations of Cascaded CNN are as follows: 1) it is more dedicated to ground-truth generation than an automated background/foreground separation method, and 2) it is also computationally expensive.

Lim and Keles [114] proposed a method called FgSegNet-M²⁰ based on a triplet CNN and a Transposed Convolutional Neural Network (TCNN) attached at the end of it in an encoder-decoder structure. Practically, the four blocks of the pre-trained VGG-16 [175] Net is employed at the beginning of the proposed CNNs under a triplet framework as the multiscale feature encoder. Furthermore, a decoder network is integrated at the end of it to map the features to a pixel-level foreground probability map. Then, a threshold is applied to this map to obtain binary segmentation labels. Practically, Lim and Keles [114] generated scene specific models using only a few frames (to 50 up to 200) similar to Wang et al. [204]. Experimental results [114] show that TCNN outperforms both ConvNet [22] and Cascaded CNN [204], and practically outperformed all the reported methods by an overall F-Measure of 0.9770. In a further work, Lim and Keles [115] designed a variant of FgSegNet-M called FgSegNet-S by adding a feature pooling module FPM which operates on top of the final encoder (CNN) layer. In an additional work, Lim et al. [116] proposed a modified FM with feature fusion. This last version called FgSegNet-V2²¹ ranked as number one on the CDnet 2014 dataset.

These previous methods usually require a large amount of densely labeled video training data. To solve this problem, Liao et al. [112] designed a multi-scale cascaded scene-specific (MCSS) CNNs based background subtraction method with a novel training strategy. The architecture combined the ConvNets [22] and the multiscale-cascaded architecture [204] with a training that takes advantage of the balance of positive and negative training samples. Experimental results show that MCSS outperforms Deep CNN [4], TCNN [226] and SFEN [32] with a score of 0.904 on the CDnet 2014 dataset by excluding the PTZ category.

Liang et al. [111] developed a multi-scale CNN based background subtraction method by learning a specific CNN model for each video to ensure accuracy, but manage to avoid manual labeling. First, Liang et al. [111] applied the SubSENSE algorithm to get an initial foreground mask. Then, an adaptive strategy is applied to

select reliable pixels to guide the CNN training because the outputs of SubSENSE cannot be directly used as ground truth due the lack of accuracy of the results. A simple strategy is also proposed to automatically select informative frames for the guided learning. Experiments on the CDnet 2014 dataset show that Guided Multi-scale CNN gives a better F-Measure of 0.7591 than DeepBS [4] and SuBSENSE [178].

4.3 Fully CNNs

Cinelli [37] proposed a similar method than Braham and Droogenbroeck [22] by exploring the advantages of Fully Convolutional Neural Networks (FCNNs) [119] to diminish the computational requirements. FCNN use convolutional layer to replace the fully connected layer in traditional convolution networks, which can avoid the disadvantages caused by fully connection layer. Practically, Cinelli tested both LeNet5 [43] and ResNet [73] architectures. As the ResNet presents a greater degree of hyperparameter setting (namely the size of the model and even the organization of layers) compare to LeNet5, Cinelli also varied different features of the ResNet architectures to optimize them for background/foreground separation. For this, Cinelli used the networks designed for the ImageNet Large Scale Visual Recognition Challenge (ILSVRC²²), which deal with 224×224 pixel images, and those for the CIFAR-10 and CIFAR-100 datasets²³, which have 32×32 pixel-images as input. The FAIR²⁴ implementation is employed. From this study, the best models on the CDnet 2014 dataset [203] are the 32-layer CIFAR-derived dilated network and the pre-trained 34-layer ILSVRC-based dilated model adapted by direct substitution. But, Cinelli [37] only provided visual results without F-measure.

In another work, Yang et al. [216] also used FCNN but with a structure of shortcut connected block with multiple branches. Each block provides four different branches. Practically, the front of three branches calculate different features by using different atrous convolution, and the last branch is the shortcut connection. For the spatial information, atrous convolution [75] is employed instead of common convolution in order to miss considerable details by expanding the receptive fields. For the activation layers, PReLU Parametric Rectified Linear Unit (PReLU) [74] introduced a learned parameter to transform the values less than 0. Yang et al. [216] also employed a refinement method using Conditional Random Fields (CRF). Experimental results show that this method outperforms traditional background subtraction methods (MOG [180] and Codebook [209]) as well as recent state-of-art methods (ViBe [11], PBAS [81] and P2M [215]) on the CDnet 2012 dataset [62]. But, Yang et al.

¹⁷<https://github.com/zhimingluo/MovingObjectSegmentation/>

¹⁸<http://caffe.berkeleyvision.org/tutorial/solver.html>

¹⁹<http://www.vlfeat.org/matconvnet/>

²⁰<https://github.com/lim-anggun/FgSegNet>

²¹<https://github.com/lim-anggun/FgSegNet-v2>

²²<http://www.image-net.org/challenges/LSVRC/>

²³<https://www.cs.toronto.edu/~kriz/cifar.html>

²⁴<https://github.com/facebook/fb.resnet.torch>

[216] evaluated their method on a subset of 6 sequences of CDnet 2012 [62] instead of all the categories of CDnet 2014 [203] making the comparison more difficult with the other DNN methods.

Alikan [2] designed a Multi-View receptive field Fully CNN (MV-FCN) based on fully convolutional structure, inception modules [185], and residual networking. MV-FCN is based on inception module [184] designed by Google that performs convolution of multiple filters with different scales on the same input to simulate human cognitive processes in perceiving multi-scale information, and ResNet [73] developed by Microsoft that acts as lost feature recovery mechanism. In addition, Alikan [2] exploits intra-domain transfer learning that boosts the correct foreground region prediction. Practically, MV-FCN employs inception modules at early and late stages with three different sizes of receptive fields to capture invariance at various scales. The features learned in the encoding phase are fused with appropriate feature maps in the decoding phase through residual connections for achieving enhanced spatial representation. These multi-view receptive fields and residual feature connections provide generalized features for a more accurate pixel-wise foreground region identification. The training is made with the CDnet 2014 [203]. Alikan et al. [2] evaluated MV-FCN against classical neural networks (Stacked Multi-Layer [227], Multi-Layered SOM [59]), and two deep learning approaches (SDAE [222], Deep CNN [4]) on the CDnet 2014 [203] but only on selected sequences making the comparison less complete.

Zeng and Zhu [221] developed a Multiscale Fully Convolutional Network (MFCN) for moving object detection in infrared videos. MFCN does not need to extract the background images. The input is frames from different sequences, and the output is a probability map. Practically, Zeng and Zhu [221] used the VGG-16 as architecture and the inputs have a size of 224×224 . The VGG-16 network is split into five blocks with each block containing some convolution and max pooling operations. The lower blocks have a higher spatial resolution and contain more low-level local features whilst the deeper blocks contain more high-level global features at a lower resolution. A contrast layer is added behind the output feature layer based on the average pooling operation with a kernel size of 3×3 . In order to exploit multi-scale features from multiple layers, Zeng and Zhu [221] employed a set of deconvolution operations to up-sample the features, creating an output probability map the same size as the input. For the loss function, the cross-entropy is used. The layers from VGG-16 are initialized with pre-trained weights, whilst the other weights are randomly initialized with a truncated normal distribution. The adam optimizer method is used for updating the model parameters. Experimental results on the THM category of CDnet 2014 [203] show that MFCN obtains the best score in this category with 0.9870 while Cascaded CNN [204] obtains 0.8958 whilst MFCN achieves a score of 0.96 over all the categories. In a further work, Zeng and Zhu [220] fused the results produced by different background subtraction algorithms (SuBSENSE [178], FTSG [200], and CwisarDH+ [65]) in order to output a more precise result. This method called CNN-SFC outperforms its direct competitor IUTIS [14] on the CDnet 2014 dataset.

Lin et al. [117] designed a deep Fully Convolutional Semantic Network (FCSN) for background subtraction. First, FCN is able to learn the global differences between the foreground and the background. Second, SuBSENSE [178] algorithm is

employed to generate robust background image with better performance, which is concatenated into the input of the network together with the video frame. Furthermore, Lin et al. [117] initialized the weights of FCSN by partially using pre-trained weights of FCN-VGG16, because these weights are applied to semantic segmentation. Then, FCSN can understand semantic information of images and converge faster. In addition, FCSN uses less training data and get better result with the help of pre-trained weights.

4.4 Deep CNNs

Babae et al. [4] proposed a deep CNNs based moving objects detection method which contains the following components: an algorithm for background initialization via an average model in RGB, a CNN model for background subtraction, and a post-processing module of the networks output using a spatial median filter. First, Babae et al. [4] proposed to distinguish the foreground pixels and background pixels with SuBSENSE algorithm [178], and then only used the background pixel values to obtain the background average model. In order to have adaptive memory length based on the motion of the camera and objects in the video frames, Babae et al. [4] used Flux Tensor with Split Gaussian Models (FTSG [200]) algorithm. For the network architecture and training, Babae et al. [4] trained the CNNs with background images obtained by the SuBSENSE algorithm [178]. With images of size 240×320 pixels, the network is trained with pairs of RGB image patches (triplets of size 37×37) from video, background frames and the respective ground truth segmentation patches (CDnet 2014 [203] with around 5% of the data). Thus, instead of training a network for a specific scene, Babae et al. [4] trained their model all at once by combining training frames from various video sequences including 5% of frames from each video sequence. On the other hand, the same training procedure than ConvNet [22] is employed. Each image-patches are combined with background-patches then fed to the network. The network contains 3 convolutional layers and a 2-layer Multi-Layer Perceptron (MLP). Rectified Linear Unit (ReLU) [142] is used as activation function after each convolutional layer and the sigmoid function after the last fully connected layer. In addition, batch normalization layers are used before each activation layer to decrease over-fitting and to also provide higher learning rates for training. Finally, a spatial-median filtering is applied in the post-processing step. This method provided foreground mask more precise than ConvNet [22] and not very prone to outliers in presence of dynamic backgrounds. Finally, deep CNN based background subtraction outperforms the existing algorithms when the challenge does not lie in the background modeling maintenance. Deep CNN obtained an F-Measure of 0.7548 in CDnet2014 dataset [203]. The limitations of Deep CNN are as follows: 1) It can not well handle the camouflage regions within foreground objects, 2) it provided poor performance for PTZ videos, and 3) due to the corruption of the background images, it performs poorly in presence of large changes in the background.

In a further work, Zhao et al. [226] proposed an end-to-end two-stage deep CNN (TS-CNN) framework. In the first stage, a convolutional encoder-decoder sub-network

is used to reconstruct the background images and encode rich prior knowledge of background scenes whilst the reconstructed background and current frame are the inputs into a Multi-Channel Fully-Convolutional sub-Network (MCFCN) for accurate foreground detection in the second stage. In the two-stage CNN, the reconstruction loss and segmentation loss are jointly optimized. Practically, the encoder contains a set of convolutions, and represents the input image as a latent feature vector. The decoder restores the background image from the feature vector. The l_2 loss was employed as the reconstruction loss. After training, the encoder-decoder network separates the background from the input image and restores a clean background image. The second network can learn semantic knowledge of the foreground and background. Therefore, it could handle various challenges such as the night light, shadows and camouflaged foreground objects. Experimental results [226] show that the TS-CNN outperforms SuBSENSE [178], PAWCS [179], FTSG [200] and Shared-Model [31] in the case of night videos, camera jitter, shadows, thermal imagery and bad weather. In CDnet2014 dataset [203], TS-CNN and Joint TS-CNN obtained an F-Measure of 0.7870 and 0.8124, respectively.

In another approach, Li et al. [110] designed an adaptive deep CNN (ADCNN) to predict object locations in a surveillance scene. First, the generic CNN-based classifier is transferred to the surveillance scene by selecting useful kernels. Secondly, the context information of the surveillance scene is learned in the regression model for accurate location prediction. Our main contributions. ADCNN achieved very interesting performance on several surveillance datasets for pedestrian detection and vehicle detection but ADCNN focus on object detection and thus not use the principle of background subtraction. Furthermore, Li et al. [110] provided results with the CUHK square dataset [199], the MIT traffic dataset [202] and the PETS 2007²⁵ instead of the CDnet2014 dataset [203].

In another work, Chen et al. [32] proposed to detect moving objects via an end-to-end deep sequence learning architecture with the pixel-level semantic features. Video sequences are the input into a deep convolutional encoder-decoder network to extract pixel-level semantic features. Practically, Chen et al. [32] used the VGG-16 [175] as encoder-decoder network but other architectures, such as GoogLeNet [185], ResNet50 [73] can be also used into this framework. An attention long short-term memory model named Attention ConvLSTM is used to integrate pixel-wise changes over time. After, a Spatial Transformer Network (STN) model and a Conditional Random Fields (CRF) layer are employed to reduce the sensitivity to camera motion and to smooth the foreground boundaries, respectively. Experimental results [32] on the two large-scale dataset CDnet 2014 dataset [203] and LASIESTA [41] show that the proposed method obtained similar results than Convnet [22] with better performance for the category "Night videos", "Camera jitter", "Shadow" and "Turbulence". Attention ConvLSTM obtained an F-Measure of 0.8292 with VGG-16, 0.7360 with GoogLeNet and 0.8772 with ResNet50.

²⁵<http://www.cvg.reading.ac.uk/pets2007/data.html>

4.5 Structured CNNs

Lim et al. [113] developed an encoder-decoder structured CNN (Struct-CNN) for background subtraction. Thus, the background subtraction model involves the following components: a background image extraction via a temporal median in RGB, network training, background subtraction and foreground extraction based on superpixel information. The structure is similar to the VGG16 network [175] after excluding the fully connected layers. The encoder converts the 3 (RGB) channel input (images of size 336×336 pixels) into 512-channel feature vector through convolutional and max-pooling layers yielding a $21 \times 21 \times 512$ feature vector. Then, the decoder converts the feature vector into a 1-channel image of size 336×336 pixels providing the foreground mask through deconvolutional and unpooling layers. Lim et al. [113] trained this encoder-decoder structured network in the end-to-end manner using CDnet 2014 [203]. For the architecture, the decoder consists of 6 deconvolutional layers and 4 unpooling layers. In all deconvolutional layers, except for the last one, features are batch-normalized and the Parametric Rectified Linear Unit (PReLU) [75] is employed as an activation function. The last deconvolutional layer which is the prediction layer used the sigmoid activation function to normalize outputs and then to provide the foreground mask. 5×5 kernels are used in all convolutional while a 3×3 kernel is employed in the prediction layer. In order to suppress the incorrect boundaries and holes in the foreground mask, Lim et al. [113] used the superpixel information obtained by an edge detector. Experimental results [113] show that Struct-CNN outperforms SuBSENSE [178], PAWCS [179], FTSG [200] and SharedModel [31] in the case of bad weather, camera jitter, low frame rate, intermittent object motion and thermal imagery. Struct-CNN obtained an F-Measure of 0.8645 on the CDnet 2014 dataset [203] excluding the "PTZ" category. Lim et al. [113] excluded this category arguing that they focused only on static cameras.

4.6 3D-CNNs

Sakkos et al. [161] designed an end-to-end 3D-CNN to track temporal changes in video sequences avoiding the use of a background model for the training. 3D-CNN can handle multiple scenes without further fine-tuning on each scene individually. For the architecture, Sakkos et al. [161] used C3D branch [190]. Experimental results [161] reveal that 3D-CNN provides better performance than ConvNet [22] and deep CNN [4]. Furthermore, experiments on the ESI dataset [196] which present extreme and sudden illumination changes, show that 3D-CNN outperforms two designed illumination invariant background subtraction methods that are Universal Multimode Background Subtraction (UMBS) [160] and ESI [196]. 3D-CNN obtained an average F-Measure of 0.9507 in CDnet 2014 dataset.

Yu et al. [218] employed a spatial-temporal attention-based 3D ConvNets to jointly model the appearance and motion of objects-of-interest in a video for a Relevant Motion Event detection Network (ReMotENet). The architecture is based on the C3D branch [190]. But, instead of using max pooling both spatially and tem-

porally, Yu et al. [218] separated the spatial and temporal max pooling in order to capture fine-grained temporal information, and makes the network deeper to learn better representations. Experiments demonstrate that ReMotENet achieves comparable or even better performance, but is three to four orders of magnitude faster than the object detection based method. It can detect relevant motion in a 15s video in 4 – 8 milliseconds on a GPU and a fraction of second on a CPU with model size of less than 1MB.

In another work, Hu et al. [82] developed a 3D atrous CNN model to learn deep spatial-temporal features without losing resolution information. In addition, this model is combined with two convolutional long short-term memory (ConvLSTM) networks in order to capture both short-term and long-term spatio-temporal information of the input video data. Furthermore, 3D Atrous ConvLSTM is a completely end-to-end framework that doesn't require any pre- or post-processing of the data. Experiments on CDnet 204 dataset show that 3D atrous CNN outperforms SuBSENSE [179], Cascaded CNN [204] and DeepBS [4].

4.7 CNNs with Different Features

4.7.1 Random Permutation of Temporal Pixels (RPoTP) feature

Zhao et al. [224] designed a Deep Pixel Distribution Learning (DPDL) model for background subtraction. For the input of the CNNs, Zhao et al. [224] employed a feature named Random Permutation of Temporal Pixels (RPoTP) features instead of using the intensity values as in the previous methods. RPoTP is used to represent the distribution of past observations for a particular pixel, in which the temporal correlation between observations is deliberately no ordered over time. Then, a convolutional neural network (CNN) is used to learn the distribution for determining whether the current observation is foreground or background. The random permutation allows the framework to focus primarily on the distribution of observations, rather than be disturbed by spurious temporal correlations. For a large number of RPoTP features, the pixel representation is captured even with a small number of ground-truth frames. Experiments on the CDnet 2014 dataset show that DPDL is effective even with only a single ground-truth frame giving similar performance than the MOG model in this case. With 20 GTs, DPDL obtains similar scores than SubSENSE [179]. Finally, DPDL²⁶ with 40 GTs gives an average F-Measure of 0.8106 outperforming DeepBS [4].

4.7.2 Depth feature

Wang et al. [201] proposed a BackGround Subtraction neural Networks for Depth videos (BGSNet-D) to detect moving objects in the scenarios where color information are unable to get. Thus, BGSNet-D is suitable in the dark scenes, where color in-

²⁶<https://github.com/zhaochenqiu/DPDL>

formation is hard to obtain. CNNs can extract features in color images, but cannot be applied to depth images directly because there exists edge noise and pixel absence in the captured data. To address this problem, Wang et al. [201] designed an extended min-max normalization method to pre-process the depth images. After pre-processing, the two inputs of the CNNs are the average background image in depth and the current image in depth. Then the architecture is similar to ConvNets with three convolutional layers. In each convolutional layer, a filter with 3×3 local receptive fields and a 1×1 stride is used. ReLU follows as the activation function in hidden layers. Batch normalization layer and pooling layer are after each ReLU layer. Finally, all feature maps are employed as inputs of a Multilayer Perceptron (MLP) which contains three fully connected layers. Sigmoid is used as activation function and the output only consists of a single unit. Experiments on the SBM-RGBD²⁷ dataset [25] show that BGSNet-D outperforms existing methods that use only depth data, and even reaches the performance of the methods that use RGB-D data.

4.8 Generative Adversarial Networks

Bakkay et al. [10] proposed a background subtraction method based on conditional Generative Adversarial Network (cGAN). This model named BScGAN consists of two successive networks: generator and discriminator. The generator learns the mapping from the background and current image to the foreground mask. Then, the discriminator learns a loss function to train this mapping by comparing ground-truth and predicted output with observing the input image and background. For the architecture, the generator network follows an encoder-decoder architecture of Unet network with skip connections [85]. Practically, the encoder part includes down-sampling layers that decrease the size of the feature maps followed by convolutional filters. It consists of 8 convolutional layers. The first layer uses 7×7 convolution to provide 64 feature maps. The 8th layer generates 512 feature maps with a 1×1 size. Their weights are randomly initialized. In addition, the middle 6 convolutional layers are six ResNet blocks. In all encoder layers, Leaky-ReLU non-linearities are used. For the decoder part, it uses upsampling layers followed by deconvolutional filters to construct an output image with the same resolution of the input one. Its architecture is similar to the encoder one including 8 deconvolutional layers, but with a reverse layers ordering and with downsampling layers being replaced by up-sampling layers. For the discriminator network, the architecture is composed of 4 convolutional and down-sampling layers. The first layer generates 64 feature maps. Moreover, the 4th layer generates 512 feature maps with a 30×30 size. The convolutions are 3×3 spatial filters and their corresponding weights are randomly initialized. Leaky ReLU functions are employed as activation functions. Experimental results on CDnet 2014 datasets shows that BScGAN outperforms ConvNets [22], Cascaded CNN [204], and Deep CNN [4] with an average F-Measure of 0.9763 without the category PTZ.

Zheng et al. [228] employed a Bayesian GAN (BGAN) approach. First, a median filter algorithm is used to extract the background and then a network based

²⁷<http://rgbd2017.na.icar.cnr.it/SBM-RGBDdataset.html>

on Bayesian generative adversarial network is trained to classify each pixel, thereby dealing with the challenges of sudden and slow illumination changes, non-stationary background, and ghost. Practically, deep convolutional neural networks are adopted to construct the generator and the discriminator of Bayesian generative adversarial network. In a further work, Zheng et al. [230] proposed a parallel version of the BGAN algorithm named (BPVGAN).

Bahri et al. [9] designed an end-to-end framework called Neural Unsupervised Moving Object Detection (NUMOD). It is based on the batch method named IL-ISD [170]. NUMOD can work either in an online and batch mode thanks to the parametrization via the generative neural network. NUMOD decomposes each frame into three parts: background, foreground and illumination changes. It uses a fully connected generative neural network to generate a background model by finding a low-dimensional manifold for the background of the image sequence. For the architecture, NUMOD uses two Generative Fully Connected Networks (GFCN). Net1 estimates the background image from the input image while Net2 generates background image from the illumination invariant image. These two networks have the exact same architecture. Thus, the input to GFCN is an optimizable low-dimensional latent vector. Then, two fully connected hidden layers are followed by ReLU non-linearity. The second hidden layer is fully connected to the output layer which is followed by the sigmoid function. A loss term is employed to impose the output of GFCN to be similar to the current input frame. Practically, GFCN is similar to the decoder part of an auto-encoder. In an auto-encoder, the low dimensional latent code is learned by the encoder, whilst in GFCN, it is a free parameter that can be optimized and is the input to the network. During training, this latent vector learns a low-dimensional manifold of the input distribution.

5 Deep Learned Features

Features used played an important role in the robustness against the challenge met in video [19]. Historically, low-level and hand-craft features such as color [120][169], edge [40][101], texture [77][172], motion [61][136], and depth [3][23][24][55][88][141] features were often employed to deal with illumination changes, dynamic background, and camouflage. But, it needs practically to choose an operator [5][7][35] to fuse the results which come from the different features or a feature selection scheme [173][174]. Nevertheless, none of these approaches can finally compete with approaches based on deep learned features.

5.1 Stacked Denoising AutoEncoders

Zhang et al. [222] designed a deep learned features based block-wise method with a binary spatio-temporal background model. Based on the Stacked Denoising AutoEncoder (SDAE), the deep learning module learns a deep image representation encoding the intrinsic scene information. This leads to the robustness of feature description.

Furthermore, the binary background model captures the spatio-temporal scene distribution information in the Hamming space to perform foreground detection. Experimental results [222] on the CDnet 2012 dataset [62] demonstrate that SDAE gives better performance than traditional methods (MOG [180], KDE [49], LBP [77]), and recent state-of-art model (PBAS [81]). To address robustness against stationary noise, Garcia-Gonzalez [57] also used a stacked denoising autoencoders to generate a set of robust features for each patch of the image. Then, this set is considered as the input of a probabilistic model to determine if that region is background or foreground.

5.1.1 Neural Reponse Mixture

Shafiee et al. [166][167] proposed a Neural Reponse Mixture (NeRM) framework to extract rich deep learned features with which to build a reliable MOG background model. Practically, the first synaptic layer of StochasticNet [168] is trained on the ImageNet dataset [45] as a primitive, low-level, feature representation. Thus, the neural responses of the first synaptic layer at all pixels in the frame is then used as a feature to distinguish motion caused by objects moving in the scene. It is worth noting that the formation of StochasticNets used in the NeRM framework is a one-time and off-line procedure which is not implemented on an embedded system. The final formed StochasticNet is transferred to the embedded system. Then, MOG model is employed using the deep learned features. Experimental results [166] on the CDnet 2012 dataset [62] show that MOG-NeRM globally outperforms both the MOG model with RGB features and Color based Histogram model called CHist [30], but gives not the best score for the following categories: "intermittentObjectMotion", "Low frame rate", "Night video", and "Thermal".

5.2 Motion Feature Network

Nguyen et al. [143] combined a sample-based background model with a feature extractor obtained by training a triplet network. This network is constructed by three identical CNN, each of which is called a Motion Feature Network (MF-Net). Thus, each motion patterns is learned from small image patches and each input images of any size is transformed into feature embeddings for high-level representations. A sample based background model is then used with the color feature and the extracted deep motion features. To classify whether a pixel is background or foreground, Nguyen et al. [143] employed the l_1 distance. Furthermore, an adaptive feedback scheme is also employed. The training is made with the CDNet 2014 dataset [203] and the offline trained network is then used on the fly without re-training on any video sequence before each execution. Experimental results [143] on BMC 2012 dataset and CDNet 2014 dataset [203] show that MF-Net outperforms SOBS, LOBSTER and SuBSENSE in the case of dynamic backgrounds. Lee and Kim [108] proposed a method to learn the pattern of the motions using the Factored 3-Way Restricted Boltzmann Machines (RBM) [157] and obtain the global motion from the sequential

images. Once this global motion is identified between frames, background subtraction is achieved by selecting the regions that do not respect the global motion. These regions are thus considered as the foreground region

6 Adequacy for the background subtraction task

All the previous works demonstrated the performance of DNN for background subtraction but not discuss the reason why DNN works well. A first way to analyze these performance is to compare these different methods. For this, we have grouped in Table 3 a comparative overview of the architectures while we show an overview in terms of the challenges in Table 4. From Table 3, we can see that it is possible to have three type of input: current image only, background and current images. In the first case, the authors works either with the current images without computing a background image or with a end-to-end solution that first generates a background image. In the second case, the authors have to compute the background image by using the temporal median or another model like SuBSENSE. The output is always the foreground mask except for NUMOD which provide the background and the foreground mask but also an illumination change mask. For the architecture, most of the authors employed a well-know architecture (LeNet-5, VGG-16 and U-Net) that they slightly adapted to the task of background subtraction. Only few authors proposed a full designed architecture for background subtraction. Table 4 groups the solutions of the different methods for the limitations of ConvNets [22]. To learn the process at different level, the most common solutions are multi-scale and cascaded strategies alleviating the drawback to work with patches. For the training, over-fitting is often the case producing scene-specific methods. For the dataset used for the training, most of the authors employed the CDnet 2014 dataset with a part devoted to the training phase and another part for the testing phase. End-to-end solutions are well proposed as well as spatial and temporal strategies. Most of the time, the architecture is a generative one even if a combination of generative and discriminative would be better suitable for background subtraction. Indeed, the background modeling is more a reconstructive task while the foreground detection is more a discriminative task.

To analyze how and why the DNN works well for this application, Minematsu et al. [134][135] provided a valuable analysis by testing a quasi-similar method than ConvNet [22] and found that the first layer performs the role of background subtraction using several filters whilst the last layer categorizes some background changes into a group without supervised signals. Thus, DNN automatically discovers background features through feature extraction by background subtraction and the integration of the features [134] showing its potential for background/foreground separation. This first analysis is very valuable but the adequacy of a DNN method for the application of background/foreground separation should also be investigated in other key issues, that are the challenges and requirements met in background subtraction, and the adequacy of the architecture for background subtraction.

To be effective, a background/foreground separation method should addressed the challenges and requirements met in this application, that are (1) its robustness to noise, (2) its spatial and temporal coherence, (3) the existence of an incremental

version, (4) the existence of a real-time implementation, and (5) the ability to deal with the challenges met in video sequences. Practically, issue (1) is ensured for deep learning methods as DNN learn deep features of the background and the foreground during the training phase. For issue (2), spatial and temporal processing need to be added to pixel-wise DNN methods because, as explained in Alikan [2], one of the main challenges in DNN methods is dealing with objects of very different scales and the dithering effect at bordering pixels of foreground objects. In literature, several authors added spatial and temporal constraints via several spatial and/or temporal strategies. These strategies can be either incorporated in an end-to-end solution or can be done via a post-processing applied to the foreground mask. For example, Cascaded CNN [204] and MV-FCN [2] employed a multi-scale strategy while DeepBS [4] used a spatial median filter. Struct-CNN [113] is based on a superpixel strategy whilst Attention ConvLSTM+CRF [113] with Conditional Random Field (CRF). In another manner, Sakkos et al. [161] used directly 3D-CNN for temporal coherence while Chen et al. [32] used a spatial and temporal processing in Attention ConvLSTM. For issue (3), there is no need to update the background model in DNN methods if the training is sufficiently large to learn all the appearances of the model in terms of illumination changes and dynamics (waving trees, water rippling, waves, etc.), otherwise it is required. In this last case, several authors employed an end-to-end solution in which a DNN method for background generation is used to determine the background image over time. Then, the output of this DNN based background generation is the input of the DNN based background subtraction with the current image in order to determine the foreground mask. For issue (4), DNNs are time consuming without a specific GPU card and optimizer. Thus, the key point to have a suitable DNN methods for background subtraction is to have a large training dataset, additional spatial/temporal strategies, and to apply it with a specific card if possible. For issue (5) which concerns the challenges met in video sequences like illumination changes and dynamic backgrounds, the DNN can be sufficient by itself if the architecture allow to learn these changes as in several works or additional networks can be added.

For the adequacy of the architecture, it is needed to check the features of DNNs that are (1) type of architecture, and (2) parameters such as number of neurons, number of layers, etc. In literature, we can only found two works which compared different architecture for background/foreground separation: Cinelli [22] tested both LeNet5 [43] and ResNet [73] architectures while Chen et al. [32] compared the VGG-16 [175], the GoogLeNet [185], and the ResNet50 [73]. In these two works, ResNet [73] provided the best results. But, these architectures were first designed for different classification tasks with the ImageNet dataset [104], CIFAR-10 dataset or ILSVRC 2015 dataset but not for the background/foreground separation task with the corresponding dataset such as CDnet 2014 dataset.

7 Experimental results

For comparison, we present the results obtained on the well-known publicly available CDnet 2014 dataset [203] both in a qualitative and quantitative manner.

7.1 CDnet 2014 dataset and Challenges

CDnet 2014 dataset [203] was developed as part of Change Detection Workshop challenge (CDW 2014). This dataset includes all the videos from the CDnet 2012 dataset [62] plus 22 additional camera-captured videos providing 5 different categories that incorporate challenges that were not addressed in the 2012 dataset. Practically, the categories are as follows: baseline, dynamic backgrounds, camera jitter, shadows, intermittent object motion, thermal, challenging Weather, low frame-rate, night videos, PTZ and turbulence. In addition, whereas ground truths for all frames were made publicly available for the CDnet 2012 dataset for testing and evaluation, in the CDnet 2014, ground truths of only the first half of every video in the 5 new categories is made publicly available for testing. The evaluation will, however, be across all frames for all the videos (both new and old) as in CDnet 2012. All the challenges of these different categories have different spatial and temporal properties. It is important to determine what are the solved and unsolved challenges. Both CDnet 2012 and CDnet 2014 datasets allow to highlight in which situations it is difficult to provide robust foreground detection for existing background subtraction methods. The following remarks can be made as developed in [99]:

- Conventional background subtraction methods can efficiently deal with challenges met in baseline and bad weather sequences.
- Dynamic backgrounds, thermal video and camera jitter is a reachable challenge for top performing background subtraction.
- Night videos, low frame-rate, and PTZ videos represent huge challenges.

7.2 Performance Evaluation

7.2.1 Qualitative Evaluation

We compared the visual results obtained on the CDnet 2014 dataset by the different deep learning algorithms with visual results of other representative background subtraction algorithms that are: Two statistical models (MOG [180], RMOG [192]), one multi-cues model (SubSENSE [178]), and two conventional neural networks (SC-SOBS [126], AAPSA [155]). The deep learning models are the following ones: five CNNs based methods (Cascaded CNN [204], DeepBS [4], FgSegNet [114], FgSegNet-SFPM [115], FgSegNet-V2 [116]) and two GANs based methods (BSPV-GAN [230], DCP [181]). All the visual results come from the CDnet 2014 website except for DCP for which the authors kindly provided the results. We also let in the four figures the number ID as well as the name as it is provided in the CDnet 2014 website. Figure 1 show the visual results obtained by MOG, RMOG and

SuBSENSE. We can see that SuBSENSE clearly improved the foreground mask by reducing false positive and negative detections. From Figure 2, we can remark that Cascaded CNN outperforms the classical neural networks SC-SOBS and AAPSA except in the "Low-frame Rate" and "Night Videos" categories. In Figure 3, FgSegNet and FgSegNet-SFPM that are top methods in CDnet 2014 dataset visually outperforms DeepBS in the "Baseline" and "Thermal" Categories. In Figure 4, FgSegNet-V2 which is the top method in CDnet 2014 dataset is compared with GAN based methods that give similar visual results. Finally, we can remark that the foreground mask was progressively improved over time by statistical models, multi-cue models, conventional neural networks, and deep learning models in the order of quality.

7.2.2 Quantitative Evaluation

We compared the F-measures obtained by the different algorithms with the F-measures of other representative background subtraction algorithms over the complete evaluation dataset: **(A)** two conventional statistical models (MOG [180], RMOG [192]), **(B)** three advanced non-parametric models (SubSENSE [178], PAWCS [179], and Spectral-360 [165]), and **(C)** two conventional neural networks models (SOBS-CF [125], SC-SOBS [126]). Deep learning models for background separation are classified following their architecture:

- **Convolutional Neural Networks:** We grouped scores of 20 algorithms based on CNN that are two basic CNN algorithms (two variants of ConvNet [22]), six multi-scale or/and cascaded CNN algorithms (cascaded CNN [204], FgSegNet-M [114], FgSegNet-S [115], FgSegNet-V2 [116], MCSS [112], and Guided Multi-scale CNN [111]), 1 fully CNN algorithms (MFCN [221]), seven deep CNN algorithms (DeepBS [4], TS-CNN [226], Joint TS-CNN [226], five variants of Attention ConvLSTM [32]), one structured CNN algorithm (Struct-CNN [113]), and two 3D CNN algorithms (3D CNN [161], 3D Atrous CNN [82]).
- **Generative Adversarial Networks:** We grouped scores of 4 GAN algorithms: DCP [181], BScGAN [10], BGAN [228], and BPVGAN [230].

Furthermore, these algorithms can be labeled as pixel-wise, spatial-wise, temporal-wise and spatio-temporal-wise algorithms. For pixel-wise algorithms, they were directly applied by the authors to background/foreground separation without specific processing taking into account spatial and temporal constraints. In these algorithms, each pixel is processed independently based or not on the information contained in their local patch like in ConvNet [22]. Thus, they may produce isolated false positives and false negatives. For spatial-wise algorithms, these algorithms model the dependencies among adjacent spatial pixels and thus enforce spatial coherence like in Cascaded CNN [204] and MFCN [221] with a multi-scale strategy, Deep CNN (DeepBS) [4] with spatial median filtering, Struct-CNN [113] with super-pixel filtering, and Attention ConvLSTM+CRF [113] with Conditional Random Field. For temporal-wise algorithms, these algorithms model the dependencies among adjacent temporal pixels and thus enforces temporal coherence such as Joint TS-CNN [226] with background reconstruction feedback and 3D-CNN [161]. For spatio-temporal-wise algorithms, these algorithms model both the dependencies among adjacent spatial and temporal pixels and thus enforce both spatial and temporal coherence like


























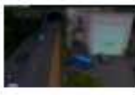





























Categories	Original	Ground Truth	4-MOGStauffer	16-MOGMiller	14-SuBSENSE
B-Weather Skating (in002349)					
Baseline Pedestrians (in000490)					
C-Jitter Badminton (in001123)					
Dynamic-B Fall (in002416)					
I-O-Motion Sofa (in001314)					
Low-F TunnelExit (in002781)					
NightVideos F-Highway (in000450)					
PIZ TwoPosition (in001216)					
Shadow BusStation (in000394)					
Thermal D-Room (in002656)					
Turbulence T-3 (in000999)					

Fig. 1 Visual results on CDnet 2014 dataset (Part 1): From left to right: Original images, Ground-Truth images, MOG (4-MOG-Stauffer [180], RMOG (16-MOGMiller [192], SubSENSE [178]).

Categories	Original	Ground Truth	10-SC-SOBS	18-AAPSA	29-Cascaded CNN
B-Weather Skating (in002349)					
Base line Pedestrians (in000490)					
C-Jitter Badminton (in001123)					
Dynamic-B Fall (in002416)					
I-O-Motion Sofa (in001314)					
Low-F TunnelExit (in002781)					
NightVideos F-Highway (in000450)					
PTZ TwoPosition (in001216)					
Shadow BusStation (in000394)					
Thermal D-Room (in002656)					
Turbulence T-3 (in000999)					

Fig. 2 Visual results on CDnet 2014 dataset (Part 2): From left to right: Original images, Ground-Truth images, SC-SOBS [126], AAPSA [155], Cascaded CNN [204].

Categories	Original	Ground Truth	34-DeepBS	39-FgSegNet	44-FgSegNet-SFPM
B-Weather Skating (in002349)					
Base line Pedestrians (in000490)					
C-Jitter Badminton (in001123)					
Dynamic-B Fall (in002416)					
I-O-Motion Sofa (in001314)					
Low-F TunnelExit (in002781)					
NightVideos F-Highway (in000450)					
PTZ TwoPosition (in001216)					
Shadow BusStation (in000394)					
Thermal D-Room (in002656)					
Turbulence T-3 (in000999)					

Fig. 3 Visual results on CDnet 2014 dataset (Part 3): From left to right: Original images, Ground-Truth images, DeepBS [4], FgSegNet [114], FgSegNetSFPM [115].

Categories	Original	Ground Truth	45-FgSegNet-V2	DCP	41-BSPVGAN
B-Weather Skating (in002349)					
Baseline Pedestrians (in000490)					
C-Jitter Badminton (in001123)					
Dynamic-B Fall (in002416)					
I-O-Motion Sofa (in001314)					
Low-F TunnelExit (in002781)					
NightVideos F-Highway (in000450)					
PTZ TwoPosition (in001216)					
Shadow BusStation (in000394)					
Thermal D-Room (in002656)					
Turbulence T-3 (in000999)					

Fig. 4 Visual results on CDnet 2014 dataset (Part 4): From left to right: Original images, Ground-Truth images, FgSegNet-V2 [116], DCP [181], BPVGAN [230]. For DCP, the authors did not tested their algorithm on four categories.

Attention ConvLSTM+PSL+CRF [32] with different architectures. Table 5 groups the different F-measures which come either from the corresponding papers or directly from changedetection.net website. Barnich and Droogenbroeck [22] did not test ConvNet on the Intermittent Motion Object (IOM) and PTZ categories because they claimed that their method is not designed for it. Similarly, Lim et al. [113] did not evaluate Struct-CNN on the PTZ category as well as MCSS and BScGAN. Zeng and Zhu [221] only evaluated MFCN on the THM category as this method is designed for infrared video. For those methods, the average F-Measure is done by indicating the missing category or the number of missing categories. For FgSegNet-M [114], FgSegNet-S [115], FgSegNet-V2 [116], we noticed that the F-Measure reported by the authors in their papers are different than the ones available on the CDnet website. We choose to report the one of the official CDnet, and the overall score provided by the authors are given between parenthesis. By analyzing Table 5, we can first see that the representative conventional neural networks Coherence-based and Fuzzy SOBS (SOBS-CF) [125] and SOBS with Spatial Coherence (SC-SOBS) [126] outperforms the basic statistical models like MOG [180] (1999) even with improvements like in RMOG [192] (2013). However, SOBS and its variants were the leader methods on the CDnet 2012 dataset [62] for a long time (around two years) showing the interest of neural networks for background subtraction. But, F-measure did not exceed 0.6 in average, that were relatively low in absolute. The F-measure exceeded only 0,9 for the baseline category making these methods only usable and reliable in applications where the environments were not too complex. Second, we can remark that advanced non parametric models as SuBSENSE [178] and PAWCS [179] developed in 2014/2015 achieved chronologically better performance than SOBS because of multi-features and multi-cues strategies. The gain in performance was around 25% for the F-Measure. The average F-measure was around 0.75 becoming to be more acceptable for a reliable use in real conditions especially that the F-measure was around 0.9 for several challenges (baseline, dynamic backgrounds, camera jitter and shadow). Thus, these methods are more applicable in more complex environments. Third, we can observe that CNNs based method can achieve a maximum gap of performance around 30% for the average F-Measure against SuBSENSE [178] and PAWCS [179] showing their superiority on this task. However, CNNs increase greatly the F-measure in the dynamic backgrounds, camera jitter, intermittent object motion and turbulence categories. For the PTZ category, the performance is mitigated as can be seen in works of several authors who did not provide results on this category arguing that they not designed their method for this challenge while score obtained by GANs are very interesting. Practically, these methods appear to be usable and reliable in a very large spectrum of environments, but there are most of the time scene-specific with a supervised mode. We can also see that the training has a great influence on the performance. Indeed, the results obtained by ConvNet using the manual foreground masks (GT) obtained a F-Measure around 0.9 while this F-Measure falls around 0.79 using the foreground masks from IUTIS showing in this case a little gap of performance in comparison with SuBSENSE [178] and PAWCS [179]. This fact also highlights that the gap of performance obtained by DNNs based methods is essentially due to their supervised aspects. In addition, their current computation times as can be seen in Table 4 are too slow to be currently employed in real applications.

Algorithms (Authors)	BSL	DBG	CJT	IOM	SHD	THM	BDW	LFR	NVD	PTZ	TBL	Average
A) Basic statistical models												
MOG (Stauffer and Grimson [180] 1999)	0.8245	0.6330	0.5969	0.5207	0.7156	0.6621	0.7380	0.5373	0.4097	0.1522	0.4663	0.5707
RMOG (Varadarajan et al. [192] 2013)	0.7848	0.7352	0.7010	0.5431	0.7212	0.4788	0.6826	0.5312	0.4265	0.2400	0.4578	0.5735
B) Advanced non parametric models												
SubSENSE (St-Charles et al. [178] 2014)	0.9503	0.8117	0.8152	0.6569	0.8986	0.8171	0.8619	0.6445	0.5599	0.3476	0.7792	0.7408
PAWCSS (St-Charles et al. [179] 2015)	0.9397	0.8938	0.8137	0.7764	0.8913	0.8324	0.8152	0.6588	0.4152	0.4615	0.6450	0.7403
Spectral-360 (Sedky et al. [165] 2014)	0.9330	0.7872	0.7156	0.5656	0.8843	0.7764	0.7569	0.6437	0.4832	0.3653	0.5429	0.7054
C) Conventional Neural Networks												
SOBS-CF (Maddalena and Petrosino [125] 2010)	0.9299	0.6519	0.7150	0.5810	0.7045	0.7140	0.6370	0.5148	0.4482	0.0368	0.4702	0.5883
SC-SOBS (Maddalena and Petrosino [126] 2012)	0.9333	0.6686	0.7051	0.5918	0.7230	0.6923	0.6620	0.5463	0.4503	0.0409	0.4880	0.5961
D) Deep Neural Networks (Structure)												
I) Convolutional Neural Networks												
I.1) Basic CNN												
CNN* (ConvNet-GT) (<i>LeNet-5</i>) (<i>Pixel-wise</i>) (Barnich and Droogenbroeck [22] 2016)	0.9813	0.8845	0.9020	-	0.9454	0.8543	0.9254	0.9612	0.7565	-	0.9297	0.9044 (IOM, PTZ)
CNN* (ConvNet-IUTIS) (<i>LeNet-5</i>) (<i>Pixel-wise</i>) (Barnich and Droogenbroeck [22] 2016)	0.9647	0.7923	0.8013	-	0.8590	0.7559	0.8849	0.8273	0.4715	-	0.7506	0.7897 (IOM, PTZ)
<i>DPDL</i> ₁ * (One GT) (<i>CNN</i>) (<i>Temporal-wise</i>) (Zhao et al. [224] 2018)	0.7886	0.6566	0.5456	0.5115	0.6957	0.6697	0.6036	0.5966	0.3953	0.2942	0.6301	0.5807
<i>DPDL</i> ₂₀ * (20 GTs) (<i>CNN</i>) (<i>Temporal-wise</i>) (Zhao et al. [224] 2018)	0.9620	0.8369	0.8627	0.8174	0.8763	0.8311	0.8107	0.6646	0.5866	0.4654	0.7173	0.7665
<i>DPDL</i> ₄₀ * (40GT) (<i>CNN</i>) (<i>Temporal-wise</i>) (Zhao et al. [224] 2018)	0.9692	0.8692	0.8661	0.8759	0.9361	0.8379	0.8688	0.7078	0.6110	0.6087	0.7636	0.8106
I.2) Multi-scale or/and Cascaded CNNs												
Cascaded CNN (<i>CNN-1/CNN-2</i>) (<i>Spatial-wise</i>) (Wang et al. [204] 2016)	0.9786	0.9658	0.9758	0.8505	0.9414	0.8958	0.9431	0.8370	0.8965	0.9168	0.9108	0.9209
FgSegNet-M (-) (<i>Spatial-wise</i>) (Lim and Keles [114] 2018)	0.9973	0.9958	0.9954	0.9951	0.9937	0.9921	0.9845	0.8786	0.9655	0.9843	0.9648	0.9770 (0.9865*)
FgSegNet-S (-) (<i>Spatial-wise</i>) (Lim and Keles [115] 2018)	0.9977	0.9958	0.9957	0.9940	0.9927	0.9937	0.9897	0.8972	0.9713	0.9879	0.9681	0.9804 (0.9878*)
FgSegNet-V2 (-) (<i>Spatial-wise</i>) (Lim et al. [116] 2018)	0.9978	0.9951	0.9938	0.9961	0.9955	0.9938	0.9904	0.9336	0.9739	0.9862	0.9727	0.9847 (0.9890*)
MCSS* (-) (<i>Spatial-wise</i>) (Liao et al. [112] 2018)	0.9940	0.881	0.794	0.770	0.915	0.883	0.861	0.725	0.788	-	0.884	0.844
Guided Multi-scale CNN* (-) (<i>Spatial-wise</i>) (Liang et al. [111] 2018)	0.9791	0.8266	0.8818	0.6229	0.8910	0.7490	0.8711	0.6396	0.5048	0.6057	0.8114	0.7591
I.3) Fully CNNs												
MFCN (-) (<i>Spatial-wise</i>) (Zeng and Zhu [221] 2018)	-	-	-	-	-	0.9870	-	-	-	-	-	0.9870 (only THM)
I.4) Deep CNNs												
Deep CNN (DeepBS) (-) (<i>Pixel-wise</i>) (Babae et al. [4] 2017)	0.9580	0.8761	0.8990	0.6098	0.9304	0.7583	0.8301	0.6002	0.5835	0.3133	0.8455	0.7548
Two-Stage CNN* (TS-CNN) (-) (<i>Pixel-wise</i>) (Zhao et al. [226] 2018)	0.9630	0.7405	0.8689	0.8734	0.9216	0.8536	0.8004	0.8075	0.6851	0.4493	0.6929	0.7870
Joint TS-CNN* (-) (<i>Temporal-wise</i>) (Zhao et al. [226] 2017)	0.9680	0.7716	0.8988	0.9066	0.9286	0.8586	0.8550	0.7491	0.7695	0.5168	0.7143	0.8124
Attention ConvLSTM* (<i>VGG-16</i>) (<i>Temporal-wise</i>) (Chen et al. [32] 2018)	0.9243	0.6030	0.9053	0.572	0.8916	0.7181	0.8493	0.5920	0.5060	0.7436	0.7347	0.7314
Attention ConvLSTM+CRF* (<i>VGG-16</i>) (<i>Spatial/Temporal-wise</i>) (Chen et al. [32] 2018)	0.9383	0.6207	0.9251	0.6058	0.8962	0.7271	0.8846	0.6113	0.5188	0.7697	0.7404	0.7489
Attention ConvLSTM+PSL+CRF* (<i>VGG-16</i>) (<i>Spatial/Temporal-wise</i>) (Chen et al. [32] 2018)	0.9594	0.7356	0.9422	0.7538	0.9084	0.8546	0.8949	0.6175	0.7526	0.7816	0.9207	0.8292
Attention ConvLSTM+PSL+CRF* (<i>GoogLeNet</i>) (<i>Spatial/Temporal-wise</i>) (Chen et al. [32] 2018)	0.8557	0.6588	0.8864	0.6488	0.8049	0.7725	0.7961	0.5947	0.6003	0.7136	0.7637	0.7360
Attention ConvLSTM+PSL+CRF* (<i>ResNet</i>) (<i>Spatial/Temporal-wise</i>) (Chen et al. [32] 2018)	0.9294	0.8220	0.9518	0.8453	0.9647	0.9444	0.9461	0.8080	0.8585	0.7776	0.8011	0.8772
I.5) Structured CNNs												
Struct-CNN* (<i>VGG-16</i>) (<i>Spatial-wise</i>) (Lim et al. [113] 2017)	0.9586	0.9112	0.8990	0.8780	0.8565	0.8048	0.8757	0.9321	0.7715	-	0.7573	0.8645
I.6) 3D CNNs												
3D CNN* (<i>C3D branch</i>) (<i>Temporal-wise</i>) (Sakkos et al. [161] 2017)	0.9691	0.9614	0.9396	0.9698	0.9706	0.9830	0.9509	0.8862	0.8565	0.8987	0.8823	0.9507
3D Atrous CNN* (ConvLTSM) (-) (<i>Spatial/Temporal-wise</i>) (Hu et al. [82] 2018)	0.9897	0.9789	0.9645	0.9637	0.9813	0.9833	0.9609	0.8994	0.9489	0.8582	0.9488	0.9615
2) Generative Adversarial Networks												
DCP* (<i>VGG-19</i>) (Sultana et al. [181] 2018)	0.8178	0.7757	0.8376	0.5979	0.7665	0.8212	0.8212	-	-	-	-	0.7620 (4)
BScGAN* (<i>UNet/ResNet</i>) (<i>Pixel-wise</i>) (Bakkay et al. [10] 2018)	0.9930	0.9784	0.9770	0.9623	0.9828	0.9612	0.9796	0.9918	0.9661	-	0.9712	0.9763 (PTZ)
BGAN (-) (<i>Pixel-wise</i>) (Zheng et al. [228] 2018)	0.9814	0.9763	0.9828	0.9366	0.9849	0.9064	0.9465	0.8472	0.8965	0.9194	0.9118	0.9339
BPVGAN (-) (<i>Pixel-wise</i>) (Zheng et al. [230] 2018)	0.9837	0.9849	0.9893	0.9366	0.9927	0.9764	0.9644	0.8508	0.9001	0.9486	0.9310	0.9501

Table 5 F-measure metric over the 6 categories of the CDnet2014, namely Baseline (BSL), Dynamic background (DBG), Camera jitter (CJT) Intermittent Motion Object (IOM), Shadows (SHD), Thermal (THM), Bad Weather (BDW), Low Frame Rate (LFR), Night Videos (NVD), PTZ, Turbulence (TBL). * indicated that the measures come from the corresponding papers otherwise the measures comes from the changedetection.net website.

8 Conclusion

In this paper, we have firstly presented a full review of recent advances on deep neural networks applied to background generation, background subtraction and deep learned features for detection of moving objects in video taken by a static camera. Experimental results on the large-scale CDnet 2014 dataset show the gap of performance obtained by the supervised deep neural networks methods in this field. Even if deep neural networks has received significant attention much more recently for background subtraction in the last two years since the seminal paper of Braham and Van Droogenbroeck [22], there are many unsolved important issues:

- The main question is what is the best suitable type of deep neural networks and its corresponding architecture for background initialization, background subtraction and deep learned features in presence of complex backgrounds?
- Looking at the experiments, several authors avoid experiments on the "PTZ" category and when the F-Measure is provided the score is not always very high. Thus, it seems that the current deep neural networks tested meet problems in the case of moving cameras.
- For the inputs, all the authors employed either gray or color images in RGB, except [224] which used a distribution learning feature improving the performance of the basic CNNs. But, it would be surely interesting to employ RGB-D images because depth information is very helpful in several challenges like camouflage as developed in Maddalena and Petrosino [130]. In addition, the conventional neural networks SOBS [131] is the top algorithm on the SBM-RGBD dataset [25]. Thus, we can expect that CNNs with RGB-D features as inputs will also achieve great performance as ForeGAN-RGBD [182] model. However, multi-spectral data would be also interesting to test. Furthermore, a study on the influence of the input feature's type would be interesting.
- Rather than working in the pixel domain, DNNs may also be applied in the measurement domain for use in conjunction with compressive sensing data like in RPCA models [44, 149].

Currently, only basic CNNs and GANs have been employed for background subtraction. Thus, future directions may investigate the adequacy and the use of pyramidal deep CNNs [191], deep belief neural networks, deep restricted kernel neural networks [183], probabilistic neural networks [58], deep fuzzy neural networks [46, 54] and fully memristive neural networks [33, 52, 71, 102, 103, 223] in the case of static camera as well as moving camera [133].

References

1. A. Agarwala, M. Dontcheva, M. Agrawala, S. Drucker, A. Colburn, B. Curless, D. Salesin, and M. Cohen. Interactive digital photomontage. *ACM Transactions on Graphics*, 23(1):294–302, 2004.
2. T. Akilan. A foreground inference network for video surveillance using multi-view receptive field. *Preprint*, January 2018.
3. L. Maddalena and A. Petrosino. Exploiting Color and Depth for Background Subtraction. *ICIAP 2017*, pages 254–265, September 2017.

4. M. Babae, D. Dinh, and G. Rigoll. A deep convolutional neural network for background subtraction. *Pattern Recognition*, September 2017.
5. F. El Baf, T. Bouwmans, and B. Vachon. Foreground detection using the Choquet integral. *International Workshop on Image Analysis for Multimedia Interactive Integral, WIAMIS 2008*, pages 187–190, May 2008.
6. F. El Baf, T. Bouwmans, and B. Vachon. Fuzzy integral for moving object detection. *IEEE International Conference on Fuzzy Systems, FUZZ-IEEE 2008*, pages 1729–1736, June 2008.
7. F. El Baf, T. Bouwmans, and B. Vachon. Fuzzy integral for moving object detection. *IEEE International Conference on Fuzzy Systems, FUZZ-IEEE 2008*, pages 1729–1736, June 2008.
8. F. El Baf, T. Bouwmans, and B. Vachon. Type-2 fuzzy mixture of Gaussians model: Application to background modeling. *International Symposium on Visual Computing, ISVC 2008*, pages 772–781, December 2008.
9. F. Bahri, M. Shakeri, and N. Ray. Online illumination invariant moving object detection by generative neural network. *Preprint*, 2018.
10. M. Bakkay, H. Rashwan, H. Salmene, L. Khoudour, D. Puig, and Y. Ruichek. BSCGAN: deep background subtraction with conditional generative adversarial networks. *IEEE International Conference on Image Processing, ICIP 2018*, October 2018.
11. O. Barnich and M. Van Droogenbroeck. ViBe: A universal background subtraction algorithm for video sequences. *IEEE Transactions on Image Processing*, 20(6):1709–1724, June 2011.
12. S. Basu, S. Mukhopadhyay, ManoharKarki, R. Bianco, S. Ganguly, R. Nemani, and S. Gayaka. Deep neural networks for texture classification: A theoretical analysis. *Neural Networks*, 97:173–182, January 2018.
13. C. Bautista, C. Dy, M. Manalac, and R. Orbe and M. Cordel. Convolutional neural network for vehicle detection in low resolution traffic videos. *TENCON 2016*, 2016.
14. S. Bianco, G. Ciocca, and R. Schettini. How far can you get by combining change detection algorithms? *CoRR*, abs/1505.02921, 2015.
15. T. Bouwmans. Background Subtraction For Visual Surveillance: A Fuzzy Approach. *Chapter 5, Handbook on Soft Computing for Video Surveillance, Taylor and Francis Group, S.K. Pal, A. Petrosino, L. Maddalena*, pages 103–139, March 2012.
16. T. Bouwmans. Traditional and recent approaches in background modeling for foreground detection: An overview. *Computer Science Review*, 11(31-66), May 2014.
17. T. Bouwmans. Traditional Approaches in Background Modeling for Video Surveillance. *Handbook Background Modeling and Foreground Detection for Video Surveillance, Taylor and Francis Group, T. Bouwmans, B. Hoferlin, F. Porikli, A. Vacavant*, July 2014.
18. T. Bouwmans, L. Maddalena, and A. Petrosino. Scene Background Initialization: a Taxonomy. *Pattern Recognition Letters*, January 2017.
19. T. Bouwmans, C. Silva, C. Marghes, M. Zitouni, H. Bhaskar, and C. Felicot. On the role and the importance of features for background modeling and foreground detection. *Computer Science Review*, 28:26–91, May 2018.
20. T. Bouwmans, A. Sobral, S. Javed, S. Jung, and E. Zahzah. Decomposition into low-rank plus additive matrices for background/foreground separation: A review for a comparative evaluation with a large-scale dataset. *Computer Science Review*, 23:1–71, February 2017.
21. T. Bouwmans and E. Zahzah. Robust pca via principal component pursuit: A review for a comparative evaluation in video surveillance. *Special Issue on Background Models Challenge, Computer Vision and Image Understanding, CVIU 2014*, 122:22–34, May 2014.
22. M. Braham and M. Van Droogenbroeck. Deep background subtraction with scene-specific convolutional neural networks. *International Conference on Systems, Signals and Image Processing, IWSSIP 2016*, pages 1–4, May 2016.
23. M. Camplani, C. Blanco, L. Salgado, F. Jaureguizar, and N. Garca. Advanced background modeling with RGB-D sensors through classifiers combination and inter-frame foreground prediction. *Machine Vision and Applications*, 2014.
24. M. Camplani, L. Maddalena, G. Moya Alcover, A. Petrosino, and L. Salgado. A Benchmarking Framework for Background Subtraction in RGBD Videos. *ICIAP 2017*, pages 219–229, September 2017.
25. M. Camplani, L. Maddalena, G. Moya Alcover, A. Petrosino, and L. Salgado. RGB-D dataset: Background learning for detection and tracking from RGBD videos. *IEEE ICIAP-Workshops 2017*, 2017.
26. E. Candès, X. Li, Y. Ma, and J. Wright. Robust principal component analysis? *International Journal of ACM*, 58(3), May 2011.

27. M. Chacon-Muguia, S. Gonzalez-Duarte, and P. Vega. Simplified SOM-neural model for video segmentation of moving objects. *International Joint Conference on Neural Networks, IJCNN 2009*, pages 474–480, 2009.
28. M. Chacon-Murguia, G. Ramirez-Alonso, and S. Gonzalez-Duarte. Improvement of a neural-fuzzy motion detection vision model for complex scenario conditions. *International Joint Conference on Neural Networks, IJCNN 2013*, August 2013.
29. L. Chen, G. Papandreou, I. Kokkinos, K. Murphy, and A. Yuille. Deeplab: Semantic image segmentation with deep convolutional nets, atrous convolution and fully connected CRFs. *arXiv preprint arXiv:1606.00915*, 2016.
30. Y. Chen, C. Chen, C. Huang, and Y. Hung. Efficient hierarchical method for background subtraction. *Pattern Recognition*, 10:40, 2007.
31. Y. Chen, J. Wang, and H. Lu. Learning sharable models for robust background subtraction. *IEEE International Conference on Multimedia and Expo, ICME 2015*, pages 1–6, 2015.
32. Y. Chen, J. Wang, B. Zhu, M. Tang, and H. Lu. Pixel-wise deep sequence learning for moving object detection. *IEEE Transactions on Circuits and Systems for Video Technology*, 2017.
33. M. Cheng, L. Xia, Z. Zhu, Y. Cai, Y. Xie, Y. Wang, and H. Yang. Time: A training-in-memory architecture for memristor-based deep neural networks. *ACM/EDAC/IEEE Design Automation Conference, DAC 2017*, pages 1–6, June 2017.
34. Y. Cheng, I. Diakonikolas, D. Kane, and A. Stewart. Robust learning of fixed-structure bayesian networks. *NIPS 2018*, 2018.
35. P. Chiranjeevi and S. Sengupta. Interval-valued model level fuzzy aggregation-based background subtraction. *IEEE Transactions on Cybernetics*, 2016.
36. F. Chollet. Keras. <https://github.com/fchollet/keras>, 2015.
37. L. Pinheiro Cinelli. Anomaly detection in surveillance videos using deep residual networks. *Master Thesis, Universidade de Rio de Janeiro*, February 2017.
38. S. Cohen. Background Estimation as a Labeling Problem. *International Conference on Computer Vision, ICCV 2005*, 2:1034–1041, October 2005.
39. C. Cortes and V. Vapnik. Support-vector networks. *Machine Learning*, 20(3):273–297, 1995.
40. C. Cuevas and N. Garcia. Tracking-based non-parametric background-foreground classification in a chromaticity-gradient space. *International Conference on Image Processing, ICIP 2010*, September 2010.
41. C. Cuevas, E. Yaeoz, and N. Garcia. Labeled dataset for integral evaluation of moving object detection algorithms: LASIESTA. *Computer Vision and Image Understanding*, 2016.
42. D. Culibrk, O. Marques, D. Socek, H. Kalva, and B. Furht. A neural network approach to Bayesian background modeling for video object segmentation. *International Conference on Computer Vision Theory and Applications, VISAPP 2006*, February 2006.
43. Y. Le Cun, L. Bottou, and P. Haffner. Gradient-based learning applied to document recognition. *Proceedings of IEEE*, 86:2278–2324, November 1998.
44. R. Davies, L. Mihaylova, N. Pavlidis, and I. Eckley. The effect of recovery algorithms on compressive sensing background subtraction. *Workshop Sensor Data Fusion: Trends, Solutions, and Applications*, 2013.
45. J. Deng, W. Dong, R. Socher, L. Li, K. Li, and L. Fei-Fei. Imagenet: A large-scale hierarchical image database. *IEEE International Conference on Computer Vision and Pattern Recognition, CVPR 2009*, 2009.
46. Y. Deng, Z. Ren, Y. Kong, F. Bao, and Q. Dai. A hierarchical fused fuzzy deep neural network for data classification. *IEEE Transactions on Fuzzy Systems*, 25(4):1006–1012, 2017.
47. Y. Dong and G. DeSouza. Adaptive learning of multi-subspace for foreground detection under illumination changes. *Computer Vision and Image Understanding*, 2010.
48. S. Elfving, E. Uchibe, and K. Doya. Sigmoid-weighted linear units for neural network function approximation in reinforcement learning. *Neural Networks*, 107:3–11, November 2018.
49. A. Elgammal and L. Davis. Non-parametric model for background subtraction. *European Conference on Computer Vision, ECCV 2000*, pages 751–767, June 2000.
50. I. Goodfellow et al. Generative adversarial networks. *NIPS 2014*, 2014.
51. M. Abadi et al. TensorFlow: Large-scale machine learning on heterogeneous distributed systems. *ACM International Conference on Multimedia*, March 2016.
52. Z. Wang et al. Fully memristive neural networks for pattern classification with unsupervised learning. *Nature Electronics*, 1:137–145, 2018.

53. D. Farcas, C. Marghes, and T. Bouwmans. Background subtraction via incremental maximum margin criterion: A discriminative approach. *Machine Vision and Applications*, 23(6):1083–1101, October 2012.
54. S. Feng and C. Chen. A fuzzy restricted boltzmann machine: Novel learning algorithms based on the crisp possibilistic mean value of fuzzy numbers. *IEEE Transactions on Fuzzy Systems*, 26(1):117–130, 2018.
55. E. Fernandez-Sanchez, L. Rubio, J. Diaz, and E. Ros. Background subtraction model based on color and depth cues. *Machine Vision and Applications*, 2014.
56. P. Fischer, A. Dosovitskiy, E. Ilg, P. Hausser, C. Hazirbas, V. Golkov, P. Smagt, D. Cremers, and T. Brox. FlowNet: Learning optical flow with convolutional networks. *arXiv preprint arXiv:1504.06852*, 2015.
57. J. Garcia-Gonzalez, J. Ortiz de Lazcano-Lobato, R. Luque-Baena, and M. Molina-Cabello. Background modeling for video sequences by stacked denoising autoencoders. *Conference of the Spanish Association for Artificial Intelligence, CAEPIA 2018*, pages 341–350, September 2018.
58. J. Gast and S. Roth. Lightweight probabilistic deep networks. *Preprint*, 2018.
59. G. Gemignani and A. Rozza. A novel background subtraction approach based on multi-layered self organizing maps. *IEEE International Conference on Image Processing*, 2015.
60. P. Gil-Jimenez, S. Maldonado-Bascon, R. Gil-Pita, and H. Gomez-Moreno. Background pixel classification for motion detection in video image sequences. *International Work Conference on Artificial and Natural Neural Network, IWANN 2003*, 2686:718–725, 2003.
61. M. Gong and L. Cheng. Incorporating estimated motion in real-time background subtraction. *IEEE International Conference on Image Processing, ICIP 2011*, pages 3265–3268, September 2011.
62. N. Goyette, P. Jodoin, F. Porikli, J. Konrad, and P. Ishwar. Changedetection.net: A new change detection benchmark dataset. *IEEE Workshop on Change Detection, CDW 2012 in conjunction with CVPR 2012*, June 2012.
63. A. Graves, A. Mohamed, and G. Hinton. Speech recognition with deep recurrent neural networks. *IEEE International Conference on Acoustics, Speech and Signal Processing*, pages 6645–6649, 2013.
64. M. Gregorio and M. Giordano. Background modeling by weightless neural networks. *SBMI 2015 Workshop in conjunction with ICIAP 2015*, September 2015.
65. M. Gregorio and M. Giordano. CwisarDH+: Background detection in RGBD videos by learning of weightless neural networks. *ICIAP 2017*, pages 242–253, 2017.
66. J. Gu, Z. Wang, J. Kuen, L. Ma, A. Shahroudy, B. Shuai, T. Liu, and X. Wang. Recent advances in convolutional neural networks. *Pattern Recognition*, 77:354–377, 2018.
67. R. Guo and H. Qi. Partially-sparse restricted Boltzmann machine for background modeling and subtraction. *International Conference on Machine Learning and Applications, ICMLA 2013*, pages 209–214, December 2013.
68. X. Guo, X. Wang, L. Yang, X. Cao, and Y. Ma. Robust foreground detection using smoothness and arbitrariness constraints. *European Conference on Computer Vision, ECCV 2014*, September 2014.
69. T. Haines and T. Xiang. Background subtraction with Dirichlet processes. *European Conference on Computer Vision, ECCV 2012*, October 2012.
70. I. Halfaoui, F. Bouzaraa, and O. Urfalioglu. CNN-Based Initial Background Estimation. *Scene Background Modeling Contest in conjunction with ICPR 2016*, 2016.
71. R. Hasan, T. Taha, and C. Yakopcic. On-chip training of memristor based deep neural networks. *International Joint Conference on Neural Networks, IJCNN 2017*, pages 3527–3534, May 2017.
72. J. He, L. Balzano, and J. Luiz. Online robust subspace tracking from partial information. *IT 2011*, September 2011.
73. K. He, X. Zhang, and S. Ren. Deep residual learning for image recognition. *IEEE Conference on Computer Vision and Pattern Recognition, CVPR 2016*, June 2016.
74. K. He, X. Zhang, S. Ren, and J. Sun. Delving deep into rectifiers: Surpassing human-level performance on imagenet classification. *IEEE International Conference on Computer Vision, ICCV 2015*, page 10261034, 2015.
75. K. He, X. Zhang, S. Ren, and J. Sun. Delving deep into rectifiers: Surpassing human-level performance on imagenet classification. *IEEE International Conference on Computer Vision, ICCV 2015*, page 10261034, 2015.
76. K. He, X. Zhang, S. Ren, and J. Sun. Deep residual learning for image recognition. *IEEE Conference on Computer Vision and Pattern Recognition, CVPR 2016*, pages 770–778, 2016.

77. M. Heikkilä and M. Pietikainen. A texture-based method for modeling the background and detecting moving objects. *IEEE Transactions on Pattern Analysis and Machine Intelligence, PAMI 2006*, 28(4):657–62, 2006.
78. G. Hinton. Deep belief nets. *NIPS Tutorial*, 2007.
79. G. Hinton, S. Osindero, and Y. Teh. A fast learning algorithm for deep belief nets. *Neural Computation*, 18(7):1527–1554, July 2006.
80. S. Hochreiter and J. Schmidhuber. Long short-term memory. *Neural Computation*, 9(8):1735–1780, 1997.
81. M. Hofmann, P. Tiefenbacher, and G. Rigoll. Background segmentation with feedback: The pixel-based adaptive segmenter. *IEEE Workshop on Change Detection, CVPR 2012*, June 2012.
82. Z. Hu, T. Turki, N. Phan, and J. Wang. 3d atrous convolutional long short-term memory network for background subtraction. *IEEE Access*, 2018.
83. J. Huang, X. Huang, and D. Metaxas. Learning with dynamic group sparsity. *International Conference on Computer Vision, ICCV 2009*, October 2009.
84. T. Huynh. Deep neural network accelerator based on fpga. *NAFOSTED 2017*, pages 254–257, 2017.
85. P. Isola, J. Zhu, T. Zhou, and A. Efros. Image to- image translation with conditional adversarial networks. *Preprint*, 2017.
86. S. Javed, T. Bouwmans, and S. Jung. Combining ARF and OR-PCA background subtraction of noisy videos. *International Conference in Image Analysis and Applications, ICIAP 2015*, September 2015.
87. S. Javed, T. Bouwmans, and S. Jung. Depth extended online RPCA with spatiotemporal constraints for robust background subtraction. *Korea-Japan Workshop on Frontiers of Computer Vision, FCV 2015*, January 2015.
88. S. Javed, T. Bouwmans, and S. Jung. Depth Extended Online RPCA with Spatiotemporal Constraints for Robust Background Subtraction. *Korea-Japan Workshop on Frontiers of Computer Vision, FCV 2015*, January 2015.
89. S. Javed, T. Bouwmans, and S. Jung. SBMI-LTD: Stationary Background Model Initialization based on Low-rank Tensor Decomposition. *ACM Symposium on Applied Computing, SAC 2017*, 2017.
90. S. Javed, T. Bouwmans, M. Sultana, and S. Jung. Moving object detection on RGBD videos using graph regularized spatiotemporal RPCA. *International Conference on Image Analysis and Processing*, pages 230–241, 2017.
91. S. Javed, A. Mahmood, T. Bouwmans, and S. Jung. Motion-Aware Graph Regularized RPCA for Background Modeling of Complex Scenes. *International Conference on Pattern Recognition, ICPR 2016*, 2016.
92. S. Javed, A. Mahmood, T. Bouwmans, and S. Jung. Spatiotemporal Low-rank Modeling for Complex Scene Background Initialization. *IEEE Transactions on Circuits and Systems for Video Technology*, 2016.
93. S. Javed, A. Mahmood, T. Bouwmans, and S. Jung. Background-Foreground Modeling Based on Spatio-temporal Sparse Subspace Clustering. *IEEE Transactions on Image Processing*, 26(12):5840–5854, December 2017.
94. S. Javed, S. Oh, T. Bouwmans, and S. Jung. Robust background subtraction to global illumination changes via multiple features based OR-PCA with MRF. *Journal of Electronic Imaging*, 2015.
95. S. Javed, A. Sobral, T. Bouwmans, and S. Jung. OR-PCA with dynamic feature selection for robust background subtraction. *ACM Symposium On Applied Computing, SAC 2015*, 2015.
96. S. Javed, A. Sobral, S. Oh, T. Bouwmans, and S. Jung. OR-PCA with MRF for Robust Foreground Detection in Highly Dynamic Backgrounds. *Asian Conference on Computer Vision, ACCV 2014*, November 2014.
97. S. Javed, A. Sobral, S. Oh, T. Bouwmans, and S. Jung. OR-PCA with MRF for robust foreground detection in highly dynamic backgrounds. *Asian conference on computer vision, ACCV 2014*, 2014.
98. Y. Jia, E. Shelhamer, J. Donahue, S. Karayev, J. Long, R. Girshick, S. Guadarrama, and T. Darrell. Caffe: Convolutional Architecture for Fast Feature Embedding. *ACM International Conference on Multimedia*, pages 675–678, 2014.
99. P. Jodoin. Motion detection: Unsolved issues and [potential] solutions. *Invited Talk, SBMI 2015 in conjunction with ICIAP 2015*, September 2015.
100. P. Jodoin, L. Maddalena, A. Petrosino, and Y. Wang. Extensive Benchmark and Survey of Modeling Methods for Scene Background Initialization. *IEEE Transactions on Image Processing*, 26(11):5244–5256, November 2017.
101. J. Kim, A. Rivera, B. Kim, K. Roy, and O. Chae. Background modeling using adaptive properties of hybrid features. *International Conference on Advanced Video and Signal-Based Surveillance, AVSS 2017*, 2017.

102. O. Krestinskaya, K. Salama, and A. James. Analog back propagation learning circuits for memristive crossbar neural networks. *IEEE International Symposium on Circuits and Systems, ISCAS 2018*, 2018.
103. O. Krestinskaya, K. Salama, and A. James. Learning in memristive neural network architectures using analog backpropagation circuits. *Preprint*, 2018.
104. A. Krizhevsky, I. Sutskever, and G. Hinton. ImageNet: Classification with Deep Convolutional Neural Networks. *International Conference on Neural Information Processing Systems, NIPS 2012*, pages 1097–1105, 2012.
105. B. Laugraud, S. Pierard, and M. Van Droogenbroeck. LaBGen-P: Apixel-level stationary background generation method based on LaBGen. *Scene Background Modeling Contest in conjunction with ICPR 2016*, 2016.
106. B. Laugraud, S. Pierard, and M. Van Droogenbroeck. A method based on motion detection for generating the background of a scene. *Pattern Recognition Letters*, 2017.
107. B. Laugraud, S. Pierard, and M. Van Droogenbroeck. LaBGen-P-Semantic: A First Step for Leveraging Semantic Segmentation in Background Generation. *MDPI Journal of Imaging*, 4(7), 2018.
108. S. Lee and D. Kim. Background subtraction using the factored 3-way restricted boltzmann machines. *Preprint*, 2018.
109. L. Li and W. Huang. Statistical modeling of complex background for foreground object detection. *IEEE Transaction on Image Processing*, 13(11):1459–1472, November 2004.
110. X. Li, M. Ye, Y. Liu, and C. Zhu. Adaptive deep convolutional neural networks for scene-specific object detection. *IEEE Transactions on Circuits and Systems for Video Technology*, September 2017.
111. X. Liang, S. Liao, X. Wang, W. Liu, Y. Chen, and S. Li. Deep background subtraction with guided learning. *IEEE International Conference on Multimedia and Expo, ICME 2018*, July 2018.
112. J. Liao, G. Guo, Y. Yan, and H. Wang. Multiscale cascaded scene-specific convolutional neural networks for background subtraction. *Pacific Rim Conference on Multimedia, PCM 2018*, pages 524–533, 2018.
113. K. Lim, W. Jang, and C. Kim. Background subtraction using encoder-decoder structured convolutional neural network. *IEEE International Conference on Advanced Video and Signal based Surveillance, AVSS 2017*, 2017.
114. L. Lim and H. Keles. Foreground segmentation using a triplet convolutional neural network for multiscale feature encoding. *Preprint*, January 2018.
115. L. Lim and H. Keles. Foreground segmentation using convolutional neural networks for multiscale feature encoding. *Pattern Recognition Letters*, 112:256–262, 2018.
116. L. Lim, I. Ang, and H. Keles. Learning multi-scale features for foreground segmentation. *Preprint*, September 2018.
117. C. Lin, B. Yan, and W. Tan. Foreground detection in surveillance video with fully convolutional semantic network. *IEEE International Conference on Image Processing, ICIP 2018*, pages 4118–4122, October 2018.
118. W. Liu, Z. Wang, X. Liu, N. Zeng, Y. Liuc, and F. Alsaadid. A survey of deep neural network architectures and their applications. *Neurocomputing*, 234:11–26, April 2017.
119. J. Long, E. Shelhamer, and T. Darrell. Fully convolutional networks for semantic segmentation. *CVPR 2015*, pages 3431–3440, 2015.
120. F. Lopez-Rubio, E. Lopez-Rubio, R. Luque-Baena, E. Dominguez, and E. Palomo. Color space selection for self-organizing map based foreground detection in video sequences. *International Joint Conference on Neural Networks, IJCNN 2014*, pages 3347–3354, July 2014.
121. C. Lu, J. Shi, and J. Jia. Online robust dictionary learning. *EURASIP Journal on Image and Video Processing, IVP 2011*, January 2011.
122. L. Maddalena and A. Petrosino. A self-organizing approach to detection of moving patterns for real-time applications. *Advances in Brain, Vision, and Artificial Intelligence*, 4729:181–190, 2007.
123. L. Maddalena and A. Petrosino. 3D neural model-based stopped object detection. *International Conference on Image Analysis and Processing, ICIAP 2009*, pages 585–593, 2009.
124. L. Maddalena and A. Petrosino. Multivalued background/foreground separation for moving object detection. *International Workshop on Fuzzy Logic and Applications, WILF 2009*, pages 263–270, June 2009.
125. L. Maddalena and A. Petrosino. Self organizing and fuzzy modelling for parked vehicles detection. *Advanced Concepts for Intelligent Vision Systems, ACVIS 2009*, pages 422–433, 2009.
126. L. Maddalena and A. Petrosino. The SOBS algorithm: What are the limits? *IEEE Workshop on Change Detection, CVPR 2012*, June 2012.

127. L. Maddalena and A. Petrosino. Stopped object detection by learning foreground model in videos. *IEEE Transactions on Neural Networks and Learning Systems*, 24(5):723–735, May 2013.
128. L. Maddalena and A. Petrosino. The 3dSOBS+ algorithm for moving object detection. *Computer Vision and Image Understanding, CVIU 2014*, 122:65–73, May 2014.
129. L. Maddalena and A. Petrosino. Background Model Initialization for Static Cameras. *Handbook on Background Modeling and Foreground Detection for Video Surveillance, CRC Press*, July 2014.
130. L. Maddalena and A. Petrosino. Background subtraction for moving object detection in rgb-d data: A survey. *MDPI Journal of Imaging*, 2018.
131. L. Maddalena and A. Petrosino. Self-organizing background subtraction using color and depth data. *Multimedia Tools and Applications*, October 2018.
132. W. McCulloch and W. Pitts. A logical calculus of the ideas immanent in nervous activity. *Bulletin of Mathematical Biophysics*, 5:115–133, 1943.
133. Y. Mehran and T. Bouwmans. New trends on moving object detection in video images captured by a moving camera: A survey. *Computer Science Review*, 28:1257–117, May 2018.
134. T. Minematsu, A. Shimada, and R. Taniguchi. Analytics of deep neural network in change detection. *IEEE International Conference on Advanced Video and Signal Based Surveillance, AVSS 2017*, September 2017.
135. T. Minematsu, A. Shimada, H. Uchiyama, and R. Taniguchi. Analytics of deep neural network-based background subtraction. *MDPI Journal of Imaging*, MDPI 2018.
136. A. Mittal. Motion-based background subtraction using adaptive kernel density estimation. *International Conference on Computer Vision and Pattern Recognition, CVPR 2004*, July 2004.
137. S. Moosavi-Dezfooli, A. Fawzi, O. Fawzi, and P. Frossard. Universal adversarial perturbations. *IEEE Conference on Computer Vision and Pattern Recognition, CVPR 2017*, July 2017.
138. S. Moosavi-Dezfooli, A. Fawzi, O. Fawzi, P. Frossard, and S. Soatto. Analysis of universal adversarial perturbations. *Preprint*, 2017.
139. K. Mopuri, U. Garg, and R. Babu. Fast feature fool: A data independent approach to universal adversarial perturbations. *British Machine Vision Conference, BMVC 2017*, 2017.
140. K. Mopuri, U. Ojha, U. Garg, and R. Babu. Nag: Network for adversary generation. *IEEE Conference on Computer Vision and Pattern Recognition, CVPR 2018*, pages 742–751, 2018.
141. G. Moya-Alcover, A. Elgammal, A. Jaume i Capo, and J. Varona. Modelling depth for nonparametric foreground segmentation using RGBD devices. *Pattern Recognition Letters*, 2016.
142. V. Nair and G. Hinton. Rectified linear units improve restricted Boltzmann machines. *International Conference on Machine Learning, ICML 2010*, 2010.
143. T. Nguyen, C. Pham, S. Ha, and J. Jeon. Change detection by training a triplet network for motion feature extraction. *IEEE Transactions on Circuits and Systems for Video Technology*, January 2018.
144. E. Nishani and B. Cico. Computer vision approaches based on deep learning and neural networks: Deep neural networks for video analysis of human pose estimation. *Mediterranean Conference on Embedded Computing, MECO 2017*, pages 1–4, 2017.
145. M. Nouiehed and M. Razaviyay. Learning deep models: Critical points and local openness. *Preprint*, 2018.
146. N. Oliver, B. Rosario, and A. Pentland. A bayesian computer vision system for modeling human interactions. *ICVS 1999*, January 1999.
147. D. Pathak, P. Krahenbuhl, J. Donahue, T. Darrell, and A. Efros. Context encoders: Feature learning by inpainting. *IEEE International Conference on Computer Vision and Pattern Recognition, CVPR 2016*, 2016.
148. P. Petersen and F. Voigtlaender. Optimal approximation of piecewise smooth functions using deep relu neural networks. *Neural Networks*, 108:296–330, December 2018.
149. S. Prativadibhayankaram, H. Luong, T. Le, and A. Kaup. Compressive online video background-foreground separation using multiple prior information and optical flow. *MDPI Journal of Imaging*, 4(7):90, June 2018.
150. J. Pulgarin-Giraldo, A. Alvarez-Meza, D. Insuasti-Ceballos, T. Bouwmans, and G. Castellanos-Dominguez. GMM Background Modeling using Divergence-based Weight Updating. *Conference Ibero-american Congress on Pattern Recognition, CIARP 2016*, 2016.
151. Z. Qu, S. Yu, and M. Fu. Motion background modeling based on context-encoder. *IEEE International Conference on Artificial Intelligence and Pattern Recognition, ICAIPR 2016*, September 2016.
152. A. Radford, L. Metz, and S. Chintala. Unsupervised representation learning with deep convolutional generative adversarial networks. *Computer Science*, 2015.

153. A. Rafique, A. Sheri, and M. Jeon. Background scene modeling for PTZ cameras using RBM. *International Conference on Control, Automation and Information Sciences, ICCAIS 2014*, pages 165–169, 2014.
154. G. Ramirez-Alonso and M. Chacon-Murguia. Self-adaptive SOM-CNN neural system for dynamic object detection in normal and complex scenarios. *Pattern Recognition*, April 2015.
155. G. Ramirez-Alonso, J. Ramirez-Quintana, and M. Chacon-Murguia. Temporal weighted learning model for background estimation with an automatic re-initialization stage and adaptive parameters update. *Pattern Recognition Letters*, 2017.
156. J. Ramirez-Quintana and M. Chacon-Murguia. Self-organizing retinotopic maps applied to background modeling for dynamic object segmentation in video sequences. *International Joint Conference on Neural Networks, IJCNN 2013*, August 2013.
157. M. Ranzato, A. Krizhevsky, and G. Hinton. Factored 3-way restricted boltzmann machines for modeling natural images. *AISTATS 2010*, 2010.
158. O. Ronneberger and T. Brox. P. Fischer. U-Net: Convolutional networks for biomedical image segmentation. *International Conference on Medical Image Computing and Computer-Assisted Intervention*, pages 234–241, 2015.
159. F. Rosenblatt. The perceptron—a perceiving and recognizing automaton. *Report 85-460-1, Cornell Aeronautical Laboratory*, 1957.
160. H. Sajid and S. Cheung. Universal multimode background subtraction. *IEEE Transactions on Image Processing*, 26(7):3249–3260, May 2017.
161. D. Sakkos, H. Liu, J. Han, and L. Shao. End-to-end video background subtraction with 3D convolutional neural networks. *Multimedia Tools and Applications*, pages 1–19, December 2017.
162. T. Salimans, I. Goodfellow, W. Zaremba, V. Cheung, A. Radford, and X. Chen. Improved techniques for training GANs. *NIPS 2016*, 2016.
163. J. Schmidhuber. Deep learning in neural networks: An overview. *Neural Networks*, pages 85–117, January 2015.
164. A. Schofield, P. Mehta, and T. Stonham. A system for counting people in video images using neural networks to identify the background scene. *Pattern Recognition*, 29:1421–1428, 1996.
165. M. Sedky, M. Moniri, and C. Chibelushi. Spectral-360: A Physics-Based Technique for Change Detection. *IEEE Change Detection Workshop, CDW 2014*, June 2014.
166. M. Shafiee, P. Siva, P. Fieguth, and A. Wong. Embedded motion detection via neural response mixture background modeling. *IEEE International Conference on Computer Vision and Pattern Recognition, CVPR 2016*, June 2016.
167. M. Shafiee, P. Siva, P. Fieguth, and A. Wong. Real-time embedded motion detection via neural response mixture modeling. *Journal of Signal Processing Systems*, June 2017.
168. M. Shafiee, P. Siva, and A. Wong. Stochasticnet: Forming deep neural networks via stochastic connectivity. *IEEE Access*, 2016.
169. A. Shahbaz, D. Hernandez, and K. Jo. Optimal color space based probabilistic foreground detector for video surveillance systems. *IEEE International Symposium on Industrial Electronics, ISIE 2017*, pages 1637–1641, 2017.
170. M. Shakeri and H. Zhang. Moving object detection in time-lapse or motion trigger image sequences using low-rank and invariant sparse decomposition. *IEEE International Conference on Computer Vision, ICCV 2017*, pages 5133–5141, 2017.
171. A. Sheri, M. Rafique, M. Jeon, and W. Pedrycz. Background subtraction using GaussianBernoulli restricted Boltzmann machine. *IET Image Processing*, 2018.
172. C. Silva, T. Bouwmans, and C. Frelicot. An eXtended center-symmetric local binary pattern for background modeling and subtraction in videos. *International Joint Conference on Computer Vision, Imaging and Computer Graphics Theory and Applications, VISAPP 2015*, March 2015.
173. C. Silva, T. Bouwmans, and C. Frelicot. Online weighted one-class ensemble for feature selection in background/foreground separation. *International Conference on Pattern Recognition, ICPR 2016*, December 2016.
174. C. Silva, T. Bouwmans, and C. Frelicot. Superpixel-based online wagging one-class ensemble for feature selection in background/foreground separation. *Pattern Recognition Letters*, 2017.
175. K. Simonyan and A. Zisserman. Very deep convolutional networks for large-scale image recognition. *International Conference on Learning Representation, ICLR 2015*, 2015.
176. A. Sobral, T. Bouwmans, and E. Zahzah. Comparison of Matrix Completion Algorithms for Background Initialization in Videos. *ICIAP 2015*, 2015.

177. N. Srivastava, G. Hinton, A. Krizhevsky, I. Sutskever, and R. Salakhutdinov. Dropout: A simple way to prevent neural networks from overfitting. *Journal of Machine Learning Research*, 15:1929–1958, June 2014.
178. P. St-Charles, G. Bilodeau, and R. Bergevin. Flexible background subtraction with self-balanced local sensitivity. *IEEE Change Detection Workshop, CDW 2014*, June 2014.
179. P. St-Charles, G. Bilodeau, and R. Bergevin. A self-adjusting approach to change detection based on background word consensus. *IEEE Winter Conference on Applications of Computer Vision, WACV 2015*, 2015.
180. C. Stauffer and E. Grimson. Adaptive background mixture models for real-time tracking. *IEEE Conference on Computer Vision and Pattern Recognition, CVPR 1999*, pages 246–252, 1999.
181. M. Sultana, A. Mahmood, S. Javed, and S. Jung. Unsupervised deep context prediction for background estimation and foreground segmentation. *Machine Vision and Applications*, October 2018.
182. M. Sultana, A. Mahmood, S. Javed, and S. Jung. Unsupervised rgb-d video object segmentation using gans. *ACCV-Workshops 2018*, December 2018.
183. J. Suykens. Deep restricted kernel machines using conjugate feature duality. *Neural Computation*, 29:2123–2163, 2017.
184. C. Szegedy, S. Ioffe, J. Shlens, and Z. Wojna. Rethinking the inception architecture for computer vision. *IEEE Conference on Computer Vision and Pattern Recognition*, pages 2818–2826, June 2016.
185. C. Szegedy, W. Liu, Y. Jia, P. Sermanet, S. Reed, D. Anguelov, D. Erhan, and A. Rabinovich. Going deeper with convolutions. *IEEE Conference on Computer Vision and Pattern Recognition, CVPR 2015*, pages 1–9, 2015.
186. C. Szegedy, W. Zaremba, I. Sutskever, J. Bruna, D. Erhan, I. Goodfellow, and R. Fergus. Intriguing properties of neural networks. *International Conference on Learning Representations*, 2014.
187. Y. Tao, P. Palasek, Z. Ling, and I. Patras. Background modelling based on generative Unet. *IEEE International Conference on Advanced Video and Signal Based Surveillance, AVSS 2017*, September 2017.
188. A. Tavakkoli. Foreground-background segmentation in video sequences using neural networks. *Intelligent Systems: Neural Networks and Applications*, May 2005.
189. K. Thekumparampil, A. Khetan, Z. Lin, and S. Oh. Robustness of conditional GANs to noisy labels. *NIPS 2018*, 2018.
190. D. Tran, L. Bourdev, R. Fergus, L. Torresani, and M. Paluri. C3D: generic features for video analysis. *IEEE International Conference on Computer Vision, ICCV 2015*, 2015.
191. I. Ullah and A. Petrosino. About pyramid structure in convolutional neural networks. *Preprint*, 2018.
192. S. Varadarajan, P. Miller, and H. Zhou. Spatial mixture of Gaussians for dynamic background modelling. *IEEE International Conference on Advanced Video and Signal Based Surveillance, AVSS 2013*, pages 63–68, 2013.
193. A. Vedaldi and K. Lenc. MatConvNet: Convolutional Neural Networks for MATLAB. <http://www.vlfeat.org/matconvnet/matconvnet-manual.pdf>, 2016.
194. R. Vidal. Mathematics of deep learning. *Seminar, Univ. La Rochelle*, 2017.
195. R. Vidal, J. Bruna, R. Giryes, and S. Soatto. Mathematics of deep learning. *Preprint*, 2018.
196. L. Vosters, C. Shan, and T. Gritti. Real-time robust background subtraction under rapidly changing illumination conditions. *Image Vision and Computing*, 30(12):10041015, 2012.
197. F. Wang, H. Liu, and J. Cheng. Visualizing deep neural network by alternately image blurring and deblurring. *Neural Networks*, 97:162–172, January 2018.
198. H. Wang, Y. Lai, W. Cheng, C. Cheng, and K. Hua. Background Extraction Based on Joint Gaussian Conditional Random Fields. *IEEE Transactions on Circuits and Systems for Video Technology*, 2017.
199. M. Wang, W. Li, and X. Wang. Transferring a generic pedestrian detector towards specific scenes. *IEEE Conference on Computer Vision and Pattern Recognition, CVPR 2012*, pages 3274–3281, 2012.
200. R. Wang, F. Bunyak, G. Seetharaman, and K. Palaniappa. Static and moving object detection using flux tensor with split Gaussian models. *IEEE International Conference on Computer Vision, CVPR 2014*, 2014.
201. X. Wang, L. Liu, G. Li, X. Dong, P. Zhao, and X. Feng. Background subtraction on depth videos with convolutional neural networks. *IEEE International Joint Conference on Neural Networks, IJCNN 2018*, pages 1–7, 2018.
202. X. Wang, X. Ma, and W. Grimson. Unsupervised activity perception in crowded and complicated scenes using hierarchical bayesian models. *IEEE Transactions on Pattern Analysis and Machine Intelligence*, 31(3):539555, March 2009.

203. Y. Wang, P. Jodoin, F. Porikli, J. Konrad, Y. Benezeth, and P. Ishwar. CDnet 2014: an expanded change detection benchmark dataset. *IEEE Workshop on Change Detection, CDW 2014 in conjunction with CVPR 2014*, June 2014.
204. Y. Wang, Z. Luo, and P. Jodoin. Interactive deep learning method for segmenting moving objects. *Pattern Recognition Letters*, 2016.
205. Z. Wang, L. Zhang, and H. Bao. PNN based motion detection with adaptive learning rate. *International Conference on Computational Intelligence and Security, CIS 2009*, pages 301–306, December 2009.
206. B. Weinstein. Scene-specific convolutional neural networks for video-based biodiversity detection. *Methods in Ecology and Evolution*, 2018.
207. B. Widrow. Generalization and information storage in networks of ADALINE. *Self Organizing Systems*, 1962.
208. B. Widrow and M. Lehr. 30 years of adaptive neural networks: perceptron, madaline, and backpropagation. *Proceedings of the IEEE*, 78(9):1415–1442, 1990.
209. M. Wu and X. Peng. Spatio-temporal context for codebook-based dynamic background subtraction. *AEU-Int. J. Electron. Commun.*, 64(8):739–747, 2010.
210. J. Xu, V. Ithapu, L. Mukherjee, J. Rehg, and V. Singh. GOSUS: Grassmannian Online Subspace Updates with Structured-sparsity. *International Conference on Computer Vision, ICCV 2013*, September 2013.
211. L. Xu, Y. Li, Y. Wang, and E. Chen. Temporally adaptive restricted Boltzmann machine for background modeling. *American Association for Artificial Intelligence, AAAI 2015*, January 2015.
212. P. Xu, M. Ye, X. Li, Q. Liu, Y. Yang, and J. Ding. Dynamic background learning through deep auto-encoder networks. *ACM International Conference on Multimedia*, November 2014.
213. P. Xu, M. Ye, Q. Liu, X. Li, L. Pei, and J. Ding. Motion detection via a couple of auto-encoder networks. *International Conference on Multimedia and Expo, ICME 2014*, 2014.
214. Y. Yan, H. Zhao, F. Kao, V. Vargas, S. Zhao, and J. Ren. Deep background subtraction of thermal and visible imagery for pedestrian detection in videos. *International Conference on Brain Inspired Cognitive Systems, BICS 2018*, 2018.
215. L. Yang, H. Cheng, J. Su, and X. Li. Pixel-to-model distance for robust background reconstruction. *IEEE Transactions on Circuits Systems and Video Technology*, 26(5):903–916, May 2016.
216. L. Yang, J. Li, Y. Luo, Y. Zhao, H. Cheng, and J. Li. Deep background modeling using fully convolutional network. *IEEE Transactions on Intelligent Transportation Systems*, 2017.
217. H. Yi, S. Shiyu, D. Xiusheng, and C. Zhigang. A study on deep neural networks framework. *IMCEC 2016*, pages 1519–1522, 2016.
218. R. Yu, H. Wang, and L. Davis. ReMotENet: efficient relevant motion event detection for large-scale home surveillance videos. *Preprint*, January 2018.
219. C. Yun, S. Sra, and A. Jadbabaie. A critical view of global optimality in deep learning. *International Conference on Machine Learning Representations, ICLR 2018*, 2018.
220. D. Zeng and M. Zhu. Combining background subtraction algorithms with convolutional neural network. *Preprint*, 2018.
221. D. Zeng and M. Zhu. Multiscale fully convolutional network for foreground object detection in infrared videos. *IEEE Geoscience and Remote Sensing Letters*, 2018.
222. Y. Zhang, X. Li, Z. Zhang, F. Wu, and L. Zhao. Deep learning driven blockwise moving object detection with binary scene modeling. *Neurocomputing*, June 2015.
223. Y. Zhang, X. Wang, and E. Friedman. Memristor-based circuit design for multilayer neural networks. *IEEE Transactions on Circuits and Systems I: Regular Papers*, 65(2):677–686, February 2018.
224. C. Zhao, T. Cham, X. Ren, J. Cai, and H. Zhu. Background subtraction based on deep pixel distribution learning. *IEEE International Conference on Multimedia and Expo, ICME 2018*, pages 1–6, 2018.
225. C. Zhao, X. Wang, and W. Cham. Background subtraction via robust dictionary learning. *EURASIP Journal on Image and Video Processing, IVP 2011*, January 2011.
226. X. Zhao, Y. Chen, M. Tang, and J. Wang. Joint background reconstruction and foreground segmentation via a two-stage convolutional neural network. *Preprint*, 2017.
227. Z. Zhao, X. Zhang, and Y. Fang. Stacked multi-layer self-organizing map for background modeling. *IEEE Transactions on Image Processing*, 2015.
228. W. Zheng, K. Wang, and F. Wang. Background subtraction algorithm based on bayesian generative adversarial networks. *Acta Automatica Sinica*, 2018.
229. W. Zheng, K. Wang, and F. Wang. Background subtraction algorithm based on bayesian generative adversarial networks. *Acta Automatica Sinica*, 2018.

230. W. Zheng, K. Wang, and F. Wang. A novel background subtraction algorithm based on parallel vision and Bayesian GANs. *Neurocomputing*, 2018.
231. Z. Zheng and P. Hong. Robust Detection of Adversarial Attacks by Modeling the Intrinsic Properties of Deep Neural Networks. *NIPS 2018*, 2018.
232. T. Zhou and D. Tao. GoDec: randomized low-rank and sparse matrix decomposition in noisy case. *International Conference on Machine Learning, ICML 2011*, 2011.
233. X. Zhou, C. Yang, and W. Yu. Moving object detection by detecting contiguous outliers in the low-rank representation. *IEEE Transactions on Pattern Analysis and Machine Intelligence*, 35:597–610, 2013.
234. Z. Zivkovic. Efficient adaptive density estimation per image pixel for the task of background subtraction. *Pattern Recognition Letters*, 27(7):773–780, January 2006.